

# **Control Oriented Modeling of the Dynamics in a Catalytic Converter**

**Master's thesis**  
performed in **Vehicular Systems**

by  
**Jenny Johansson** and **Mikaela Waller**

Reg nr: LiTH-ISY-EX-05/3707-SE

23rd September 2005



# Control Oriented Modeling of the Dynamics in a Catalytic Converter

Master's thesis

performed in **Vehicular Systems**,  
**Dept. of Electrical Engineering**  
at **Linköpings universitet**

by **Jenny Johansson** and **Mikaela Waller**

Reg nr: LiTH-ISY-EX-05/3707-SE

Supervisor: **Per Öberg**

ISY

**Richard Backman**

GM Powertrain Sweden

Examiner: **Associate Professor Lars Eriksson**

Linköpings Universitet

Linköping, 23rd September 2005



	<b>Avdelning, Institution</b> Division, Department  Vehicular Systems, Dept. of Electrical Engineering 581 83 Linköping	<b>Datum</b> Date  23rd September 2005
	<b>Språk</b> Language <input type="checkbox"/> Svenska/Swedish <input checked="" type="checkbox"/> Engelska/English  <input type="checkbox"/> _____	<b>Rapporttyp</b> Report category <input type="checkbox"/> Licentiatavhandling <input checked="" type="checkbox"/> Examensarbete <input type="checkbox"/> C-upsats <input type="checkbox"/> D-upsats <input type="checkbox"/> Övrig rapport <input type="checkbox"/> _____
<b>URL för elektronisk version</b> <a href="http://www.vehicular.isy.liu.se">http://www.vehicular.isy.liu.se</a> <a href="http://www.ep.liu.se/exjobb/isy/2005/3707/">http://www.ep.liu.se/exjobb/isy/2005/3707/</a>		
<b>Titel</b>	Modellering av dynamiken i en katalysator med avseende på reglering  Title Control Oriented Modeling of the Dynamics in a Catalytic Converter	
<b>Författare</b> Author	Jenny Johansson and Mikaela Waller	
<b>Sammanfattning</b> Abstract	<p>The legal amount of emissions that vehicles with spark ignited engines are allowed to produce are steadily reduced over time. To meet future emission requirements it is desirable to make the catalytic converter work in a more efficient way. One way to do this is to control the air-fuel-ratio according to the oxygen storage level in the converter, instead of, as is done today, always trying to keep it close to stoichiometric. The oxygen storage level cannot be measured by a sensor. Hence, a model describing the dynamic behaviors of the converter is needed to observe this level. Three such models have been examined, validated, and compared.</p> <p>Two of these models have been implemented in Matlab/Simulink and adapted to measurements from an experimental setup. Finally, one of the models was chosen to be incorporated in an extended Kalman filter (EKF), in order to make it possible to observe the oxygen storage level online.</p> <p>The model that shows best potential needs further work, and the EKF is working with flaws, but overall the results are promising.</p>	
<b>Nyckelord</b> Keywords	catalytic converter, TWC, oxygen storage, lambda, observer, EKF, modeling, simulation	



## Abstract

The legal amount of emissions that vehicles with spark ignited engines are allowed to produce are steadily reduced over time. To meet future emission requirements it is desirable to make the catalytic converter work in a more efficient way. One way to do this is to control the air-fuel-ratio according to the oxygen storage level in the converter, instead of, as is done today, always trying to keep it close to stoichiometric. The oxygen storage level cannot be measured by a sensor. Hence, a model describing the dynamic behaviors of the converter is needed to observe this level. Three such models have been examined, validated, and compared.

Two of these models have been implemented in Matlab/Simulink and adapted to measurements from an experimental setup. Finally, one of the models was chosen to be incorporated in an extended Kalman filter (EKF), in order to make it possible to observe the oxygen storage level online.

The model that shows best potential needs further work, and the EKF is working with flaws, but overall the results are promising.

**Keywords:** catalytic converter, TWC, oxygen storage, lambda, observer, EKF, modeling, simulation



## Sammanfattning

Avgasmängden som bensindrivna fordon tillåts släppa ut minskas hela tiden. Ett sätt att möta framtida krav, är att förbättra katalysatorns effektivitet. För att göra detta kan luft-bränsle-förhållandet regleras med avseende på syrelagringen i katalysatorn, istället för som idag, reglera mot stökiometriskt blandningsförhållande. Eftersom syrelagringen inte går att mäta med en givare behövs en modell som beskriver katalysatorns dynamiska egenskaper. Tre sådana modeller har undersökts, utvärderats och jämförts.

Två av modellerna har implementerats i Matlab/Simulink och anpassats till mätningar från en experimentuppställning. För att kunna observera syrelagringen online valdes slutligen en av modellerna ut, och implementerades i ett Extended Kalman filter.

Ytterligare arbete behöver läggas ner på den mest lovande modellen, och detsamma gäller för Kalmanfiltret, men på sikt förväntas resultaten kunna bli bra.

**Nyckelord:** katalysator, TWC, syrelagring, lambda, observatör, EKF, modellering, simulering



## Acknowledgement

We would like to thank our supervisor Per Öberg at Fordonssystem for all his help and rewarding discussions. We would also like to thank our examiner Lars Eriksson for interesting discussions and always being able to raise new questions. Additionally this thesis would not have existed without the help and support from Richard Backman, our supervisor at GM Powertrain Sweden.

Very special thanks go to Dr. Theophil Auckenthaler. Without your help, explanations, and answers our work would have been so much harder.

Thank you Martin Gunnarsson, for helping us in the engine laboratory, Per Andersson and the rest of the staff at Fordonssystem for the support, as well as creating the great atmosphere at Fordonssystem.

Furthermore we would like to thank Staffan and Birgitta, who have been of great help in many ways. We are especially thankful for your patience with the endless discussions about catalytic converters.

The last thanks go to our roommates Claes and Eric. Perhaps we did not hit the paper basket as often as you, but our mischiefs were definitely more entertaining.



# Notation

## Nomenclature

<i>Variable</i>	<i>Unit</i>	<i>Description</i>
$A$	$s^{-1}$	pre-exponential factor
$A_{geo}$	$m^2/m^3$	specific geometric catalyst surface
$A_{\lambda st} \dots F_{\lambda st}$	V,-	coefficients in the switch-type $\lambda$ -sensor model
$C_i$	m/s	convection mass transfer coefficient of $i$
$D_{chan}$	m	diameter gas channel
$D_{TWC}$	m	catalytic converter diameter
$E$	kJ/mol	activation energy
$K_d$	-	constant of proportionality
$K_r$	-	constant of proportionality
$K_\lambda$	-	constant of proportionality
$K_\psi$	-	constant of proportionality
$L_{TWC}$	m	TWC length
SC	$mol/m^3$	storage capacity
T	K	temperature
U	V	voltage
$V_{TWC}$	$m^3$	catalytic converter volume
$\dot{V}$	$m^3/s$	volumetric flow
$a_1 \dots a_5$	-	coefficients in the polynomial describing $N(\phi)$
$a_{\eta_{comb}}$	-	coefficient in the exhaust gas model
$b_{\eta_{comb}}$	1/K	coefficient in the exhaust gas model
$b_i$	-	triangular basis functions
$c$	$mol/m^3$	concentration
$c_p$	J/kg*K	specific heat capacity (gas phase)
$c_s$	J/kg*K	specific heat capacity (solid phase)
$f_{1,2..n}$	-	tuning parameters
$f_L$	-	function for lean input
$f_R$	-	function for rich input
$g(\zeta)$	-	function in Model B
$k$	1/s	reaction rate coefficient
$k_d$	-	parameter in Model B
$\dot{m}_f$	kg/s	fuel mass flow
$n_c$	-	number of discrete cells
$r$	-	reaction rate
$y_i$	-	mole fractions
$\Delta H$	J/mol	reaction enthalpy
$\Delta \Lambda$	-	post-catalyst AFR deviation from stoichiometric before the effect of the catalyst deactivation

$\Delta\lambda$	-	$\lambda - 1$
$\Sigma_i$	-	diffusion volumes
$\alpha$	W/m <sup>2</sup> K	heat-transfer coefficient TWC → exhaust
$\alpha_{cat}$	W/m <sup>2</sup> K	heat-transfer coefficient TWC → ambient
$\varepsilon$	-	volume fraction of gas phase
$\zeta$	-	global fraction of oxygen storage
$\eta_{CO}$	-	number of sites occupied by CO
$\eta_{comb}$	-	inverse combustion efficiency
$\theta$	-	occupancy fraction on noble metal
$\lambda$	-	normalized air-fuel-ratio
$\lambda_s$	W/m*K	heat conductivity solid phase
$\xi$	-	local fraction of oxygen storage
$\rho_s$	kg/m <sup>3</sup>	density solid phase
$\phi$	-	oxygen storage level
$\phi_{H_2/CO}$	-	H <sub>2</sub> /CO ratio
$\psi$	-	reversible catalyst deactivation

## Vectors and matrices

<i>Variable</i>	<i>Description</i>
<b>f</b>	dynamics function of state-space system
<b>h</b>	measurement function of state-space system
<b>u</b>	control vector
<b>x</b>	state vector
<b>y</b>	measurement vector
<b>v,w</b>	uncorrelated white noise process
<b>F</b>	system dynamics matrix
<b>H</b>	system measurement matrix
<b>I</b>	identity matrix
<b>K</b>	kalman gain matrix
<b>P</b>	covariance matrix of the estimate error
<b>Q</b>	covariance matrix of process white noise
<b>R</b>	covariance matrix of measurement white noise
<b>Φ</b>	fundamental matrix

## Subscripts

<i>Subscript</i>	<i>Description</i>
<i>ex</i>	excess of the species after a surface reaction has been completed
<i>exh</i>	exhaust
<i>g</i>	gas
<i>in</i>	incoming variable to the converter
<i>out</i>	outgoing variable after the converter
<i>post</i>	denotes the variable after the converter
<i>pre</i>	denotes the variable before the converter
<i>s</i>	solid
<i>tp</i>	tail-pipe
$\lambda_{st}$	switch-type $\lambda$

## Superscripts

<i>Superscript</i>	<i>Description</i>
<i>ads</i>	adsorption
<i>ch</i>	channel
<i>ox</i>	oxidation
<i>red</i>	reduction
<i>wc</i>	washcoat
*	vacant site in the catalytic converter

## Abbreviations

AFR	Air-Fuel-Ratio
FTP 75	American Federal Test Procedure
NEDC	New European Driving Cycle
O, P, R	Oxidants, Products and Reactants
ROC	Relative Oxygen coverage of Ceria
TWC	Three-Way catalytic Converter

## Constants

<i>Variable</i>	<i>Value/Unit</i>	<i>Description</i>
$\mathfrak{R}$	8.31451 J/molK	universal gas constant



# Contents

Abstract	v
Sammanfattning	vii
Acknowledgement	ix
Notation	xi
<b>1 Introduction</b>	<b>1</b>
1.1 Background . . . . .	1
1.1.1 Regulations . . . . .	1
1.1.2 Catalytic converters . . . . .	2
1.2 Purpose and method . . . . .	3
1.3 Prerequisites . . . . .	4
1.4 Thesis Outline . . . . .	4
<b>2 Model Verification Method</b>	<b>7</b>
2.1 Experimental setup . . . . .	7
2.2 Data . . . . .	8
2.3 Model adaption strategy . . . . .	9
2.4 Validation . . . . .	9
<b>3 Introduction to Emissions and Catalytic Converters</b>	<b>11</b>
3.1 Combustion Engines and Emissions . . . . .	11
3.2 The Catalytic Converter . . . . .	12
3.3 Study of the dynamics . . . . .	14
3.3.1 The sensors' influence on the measurements . . . . .	14
3.3.2 Study of the measurements . . . . .	16
<b>4 Model A - A Storage Dominated Model with ...</b>	<b>19</b>
4.1 Model . . . . .	19
4.1.1 The oxygen storage state, $\phi$ . . . . .	20
4.1.2 The reversible catalyst deactivation, $\psi$ . . . . .	21
4.1.3 Estimated $\Delta\lambda$ value after the catalytic converter . . . . .	21

4.2	Convert to switch type $\lambda$ -values . . . . .	21
4.3	Parameter Estimation . . . . .	22
4.3.1	Catalytic Converter Parameters . . . . .	23
4.3.2	Exhaust Gas and Sensor Parameters . . . . .	24
4.3.3	Parameters adjusted to the age of the converter . . . . .	24
4.4	Discussion . . . . .	24
4.4.1	The extension to switch-type $\lambda$ -values . . . . .	25
4.4.2	Validation . . . . .	26
4.4.3	Results . . . . .	27
<b>5</b>	<b>Model B - A Model Consisting of One Nonlinear...</b>	<b>31</b>
5.1	Model . . . . .	31
5.1.1	Model development . . . . .	31
5.1.2	The complete model . . . . .	34
5.1.3	Model parameters and functions . . . . .	34
5.2	Parameter estimation . . . . .	35
5.3	Validation . . . . .	36
<b>6</b>	<b>Model C - A Simplified Physical...</b>	<b>39</b>
6.1	Model . . . . .	39
6.1.1	Exhaust gas model . . . . .	39
6.1.2	TWC model . . . . .	41
6.1.3	Switch-type $\lambda$ -sensor model . . . . .	45
6.2	Parameter estimation . . . . .	46
6.2.1	Simplifications and assumption . . . . .	47
6.2.2	Estimation algorithm . . . . .	47
6.3	Validation . . . . .	48
6.3.1	The first set . . . . .	49
6.3.2	The second set . . . . .	50
6.3.3	Number of cells . . . . .	51
6.3.4	Discussion . . . . .	52
<b>7</b>	<b>Model comparison</b>	<b>53</b>
7.1	Accuracy of the models . . . . .	53
7.2	Inputs and outputs . . . . .	54
7.3	Number of states and parameters . . . . .	55
7.4	Simulation speed . . . . .	56
7.5	Extensibility . . . . .	56
7.6	Final comparison . . . . .	57
<b>8</b>	<b>Extended Kalman filter</b>	<b>59</b>
8.1	Introduction to EKF . . . . .	59
8.1.1	Parameter identification . . . . .	61
8.2	Implementation . . . . .	61
8.3	Tuning of the EKF . . . . .	62

8.4 Discussion and results . . . . .	63
8.4.1 Validation . . . . .	63
8.4.2 Properties of the EKF . . . . .	64
<b>9 Results and Discussion</b>	<b>67</b>
<b>10 Future work</b>	<b>69</b>
<b>References</b>	<b>71</b>
<b>A Chemical reactions</b>	<b>73</b>
<b>B Model A - Parameter Values</b>	<b>74</b>
<b>C Model C - Parameter Values</b>	<b>76</b>



# Chapter 1

## Introduction

### 1.1 Background

Already in 1915, concerns were raised about the risk potential of automobile pollutants, they were considered noisy, dangerous, and smelly. As a consequence the first regulation concerning emissions came in use 1959 in California and since then the allowed emission levels have been reduced. The automotive producers have a tough challenge. They do not only have to meet the emission requirements, they also want to satisfy the customers' power, fuel consumption and cost requirements, which often contradicts low emission rates.

#### 1.1.1 Regulations

In 1968, US got the first federal standards during the Clean Air Act, mainly because the smog was becoming an increasing concern. The initial targets were carbon monoxide and unburned hydrocarbons. A few years later, the adverse effect of oxides of nitrogen on the environment was recognized.

Since the first regulation, legislators all over the world have steadily reduced the legal limits of emissions over time. This is demonstrated in figure 1.1, which shows how the emission regulations for petrol vehicles in the US have changed over time.

The emission regulations are formulated as maximum values of emissions (measured in pollutant mass per distance traveled) from a vehicle following a specified driving profile, called test cycle. There are different test cycles available. Two frequently used is the American Federal Test Procedure, FTP 75, and the New European Driving Cycle, NEDC.

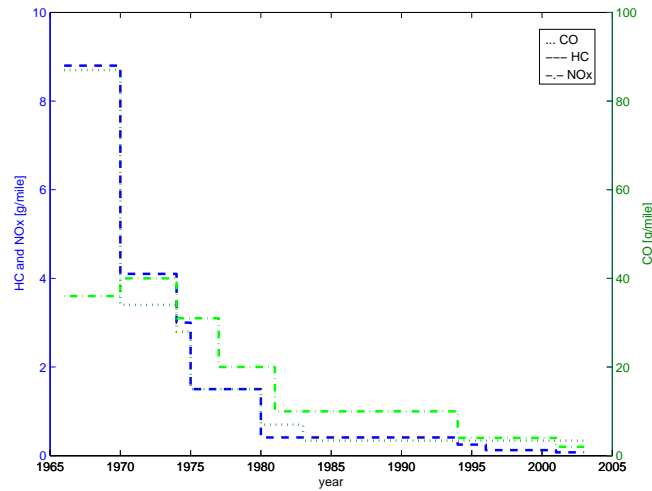


Figure 1.1: Legal limits of emissions in the US. Limits taken from [10].

### 1.1.2 Catalytic converters

The legal limits of emissions have forced the industry to accelerate the development of control systems and catalytic converters, but when the first regulation was introduced the only known way to reduce CO and HC was to lean the mixture of air and fuel. This put an end to increases in specific power outputs for a few years. During the 1970s, the two-way catalytic converters (which oxidized both CO and HCs to water and CO<sub>2</sub>) started to appear.

The most significant change in engine and catalytic converter technology came with the recognition of the adverse effect of oxides of nitrogen (NO<sub>x</sub>) on the environment. To deal with this "new" problem the combustion was carefully controlled to keep the air fuel ratio, AFR, close to stoichiometric and new catalytic converters were developed. These three-way catalytic converters (TWCs) reduce the NO<sub>x</sub> content of the exhaust gases to nitrogen as well as oxidize the HC and CO.

Although these catalytic converters were known in the early 1980s, it was not until the late 1980s that the catalytic converter became standard in new cars. Today the use of catalytic converters in exhaust after-treatment systems is essential in reducing emissions to the levels demanded by environmental legislation. Since the legislations keeps getting stronger the treatment of the pollutants has to develop as well. One way to do this is to improve the converters formulation and substrate design. Another possibility is to use advanced control and monitoring of converter operation in order to maximize the perfor-

mance.

Previously the task of the engine management system has been to keep the AFR as close to the stoichiometric value as possible which is the optimal thing to do under steady-state operating conditions. During real world driving conditions however, the AFR oscillates around the stoichiometric value. To control and optimize the engine performance with respect to emissions under transient conditions, a dynamic model of the converter is required.

Many existing models used in the design and development of catalytic converters are based on the underlying physical processes of heat transfer, chemical kinetics, and fluid dynamics, but are unsuitable for real-time control of catalytic operation because of their complexity. Up to date two types of simple dynamic models have been proposed. One based on the use of simplified chemical kinetic relationships and one based on the recognition that the catalytic converter behavior is dominated by the dynamics, storage and release, of the oxygen. Because of the limitations of the existing models, advanced converter control has not been widely implemented in practice.

## 1.2 Purpose and method

The most common way to control the emissions is to use the  $\lambda$ -sensor value before the catalytic converter to control the fuel injection time and throttle angle to get  $\lambda = 1$  and thus get the smallest amount of pollutants, (see figure 3.2).

Sometimes it is desirable to run the engine rich or lean, but this is difficult from a control point of view, since most cars cannot predict when the catalytic converter becomes unable to reduce the harmful exhausts in a satisfying way. If the converter has a high relative oxygen level, there will be no bad consequences on the exhaust if the engine runs rich for a little while, and vice versa. An advantage of this is that when the engine is running idle a lean mixture would reduce the pumping losses. Correspondingly, the turbo engine needs cooling when running at maximum load. This can be done by running the engine a little rich, since the excess fuel is reducing the temperature of the engine. The problem is that it is impossible to measure the oxygen level in the converter with a sensor. The problem can be solved by using a model of the catalytic converter and an observer that can estimate the relative oxygen level and use the relative oxygen level as input to a controller. Three such models are presented and compared in this thesis.

### 1.3 Prerequisites

To make a model of the catalytic converter and be able to use it as an observer in the engine control system, several demands have to be met. First of all the model needs to provide information about the state the catalytic converter is in, such as the oxygen storage level, and it has to be accurate enough. It also needs to be sufficiently simple to fit in the control system where CPU resources are limited. Since the dynamical behavior of a catalytic converter changes during its lifetime due to ageing, the model should be able to describe this. Finally, the model should be simple to apply and to adjust to different catalytic converters.

To be able to use the model in a control system, the output from the model needs to be comparable with measurements. Hence, a sensor model downstream of the catalytic converter might be necessary. The  $\lambda$ -sensor also has a dynamical behavior, which changes during the lifetime because of ageing, but this is neglected in this thesis. This is because the dynamics of the sensor is considerably faster than the gas composition downstream of the catalytic converter [3], and the main concern in this thesis is on the model of the catalytic converter. Furthermore, the sensor is affected largely by the same phenomenon as the catalytic converter. Hence, the dynamics of the sensor is to some extent accounted for in the model of the catalytic converter.

A study of the ageing process of the catalytic converter would require an extensive measurement process and possibly also a need for several catalytic converters of different age. There is no room for this within the scope of this thesis and it is thus not done. The ageing of the catalytic converter is accounted for by changing parameter values.

As described in section 3.2 the temperature in the catalytic converter has to reach a certain level, the light-off temperature, before the catalytic converter begins to work in a satisfying way. In this thesis, it is assumed that the engine has been running long enough to heat the catalytic converter and no steps has been done to adjust for this phenomenon.

Furthermore, the models in this thesis have been adapted to the catalytic converter in a research laboratory. Hence no considerations regarding airflow around the vehicle, changes of pressure and temperature in the ambient air etc. have been done.

### 1.4 Thesis Outline

The thesis begins with an introduction to the thesis with background, purpose, and method. The second chapter contains the model verification method, how the data has been obtained, and how to validate

the models. Chapter three presents an introduction to emissions and catalytic converters. The following three chapters describe the models investigated in this thesis, and in the seventh chapter, they are compared. In chapter eight, one of the models is incorporated in an extended Kalman filter in order to observe the oxygen storage. The results and discussion can be found in chapter nine. Finally, future work are suggested in chapter ten.



## Chapter 2

# Model Verification Method

The models described in chapter 4, 5 and 6, and the online adaption strategy in chapter 8 has been implemented in Matlab/Simulink. The measurements used to adapt and validate the models have been collected from an experimental setup.

### 2.1 Experimental setup

The experimental setup is located in the research laboratory at the division of Vehicular Systems at the Department of Electrical Engineering, Linköpings Universitet.

The engine used in this thesis is a L850 from SAAB. It is a spark ignited, four stroke, two liters, turbo charged, piston engine driven by petrol with four cylinders, much alike the engine used in SAAB 9<sup>3</sup> aero today. The control system from SAAB, Trionic 9, is a prototype system used for research. A dynamometer is used to place a load on the engine.

The catalytic converter used is of commercial type with coating of Pt and Rh.

The standard sensors mounted on the engine, as well as some additional sensors, have been used for measurements. The additional sensors are a wide-range  $\lambda$ -sensor before the catalytic converter, a switch-type  $\lambda$ -sensor after the converter, a thermocouple placed before the converter to measure the temperature of the exhaust gases and a thermocouple in the catalytic converter.

More information about the research laboratory can be found in [1] and [2].

## 2.2 Data

The measured data was chosen in roughly the same way as in [3], i.e. the  $\lambda$ -value was controlled to switch between rich (0.97) and lean (1.03), with at first 30 seconds interval, then every 15th second, every 5th, every other second, and finally every second.

In order to find the stoichiometric point the fuel injection time was tuned as the  $\lambda$ -value was controlled to switch fast between rich and lean. As shall be explained later in this thesis, a catalytic converter is able to compensate for deviation in the incoming  $\lambda$  for short periods. Hence, the stoichiometric point is found when the switch-type  $\lambda$ -sensor after the catalytic converter stays close to the switch-point. In practice this means that it is found when the sensor neither reaches the lean nor rich value, but stays somewhere in between, since a switch-type  $\lambda$ -sensor is highly nonlinear. When the stoichiometric point was found the fuel injection time was increased with 3% to make the engine run rich, and decreased with 3% to make it run lean.

The data was collected at three operating points, which can be seen in table 2.1. Two sets of data were collected at every operating point, one to use when calibrating the models, the estimation data, and the other to use when validating the models, the validation data.

<i>No.</i>	<i>Engine speed</i> <i>[rpm]</i>	<i>Engine load</i> <i>[Nm]</i>
1	1500	26
2a	1800	38
2b	1800	38
3	2500	50

Table 2.1: Operating points where measurements were taken.

At operating point number 2, two estimation and validation data sets were collected with a slight difference in the estimated position of the stoichiometric point. The switch-type  $\lambda$ -sensor values from these two data sets can be seen in figure 2.1. The dotted lines in the figure represent the rich and lean levels. This shows the great sensitivity to a very small change in the point where the AFR is assumed to be stoichiometric.

The measured wide-range  $\lambda$  before the catalytic converter at operating point number 3 can be seen in figure 2.2. The measurements in the other three sets of data look similar to this one. Notice that the wide-range  $\lambda$ -sensor before the catalytic converter suffers from a bias and show measurements between 0.98 and 1.04, even though the real  $\lambda$ -value switches between 0.97 and 1.03.

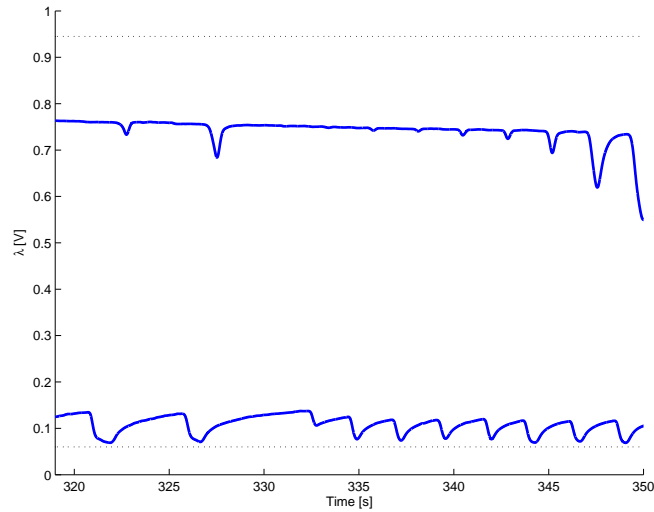


Figure 2.1: The filtered measurements from the switch-type  $\lambda$ -sensor after the catalytic converter. In both measurements, the engine is controlled to switch between rich and lean, but with a slight difference in the estimated point where the engine is assumed to run stoichiometric.

## 2.3 Model adaption strategy

The models' parameters can be adapted to the measured data by using a least-square algorithm such as the functions `fminsearch` or `lsqnonlin` in Matlab Optimization Toolbox. `fminsearch` is often more time demanding than `lsqnonlin`, but `lsqnonlin` has a higher tendency to stay in local minima.

Different variables are available to be compared to sensor signals, depending on the properties of the models.

## 2.4 Validation

One way to validate the accuracy of the catalytic converter models is to compare the  $\lambda$ -value given by the models with measured value, the effects of the sensors are important. Either a sufficiently exact sensor is required, or the use of a sensor model that is able to estimate the measured value with sufficient accuracy.

The validation can be performed by calculating the sum of the errors between the measured and simulated values. A better way however, is to compare the simulated and measured  $\lambda$ -values by looking at them. Doing this, considerations regarding the big difference in the switch-

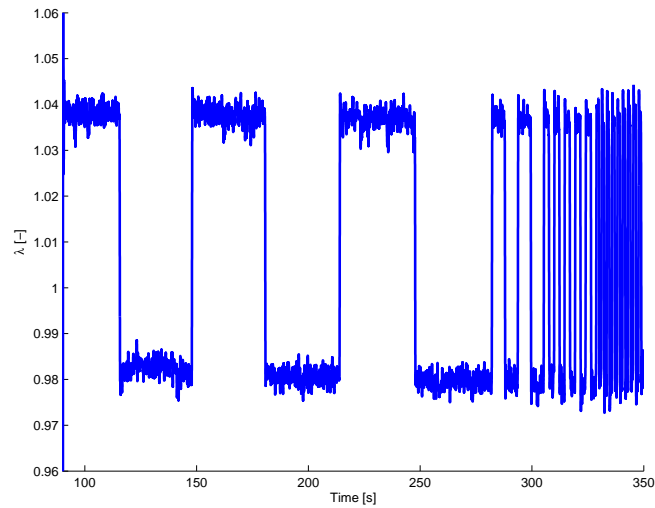


Figure 2.2: The filtered measurement from the wide-range  $\lambda$ -sensor before the catalytic converter, in one of the estimation data sets.

type sensor signal that may occur at the end of the data sets can be taken. This is due to the switch-type  $\lambda$ -sensor's high nonlinearity, as described in the previous section.

In addition the behavior of the models' states can be investigated. These are not possible to compare with measurements, but they should be examined in order to make sure they behave in a sensible way. Finally, the demand of CPU power by the models should be taken into account.

To make sure the online adaption strategy with Model C incorporated (see chapter 8) works properly, the storage capacity should be adapted to the same value after a limited amount of time, independently of the initial value. The values of the states should also be observed, to assure that they behave as predicted.

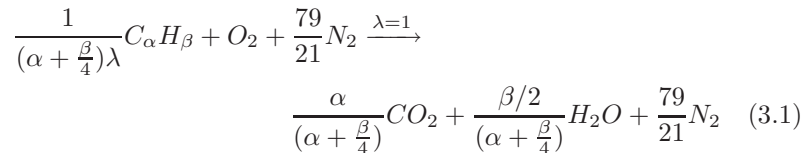
## Chapter 3

# Introduction to Emissions and Catalytic Converters

Cars are equipped with catalytic converters in order to reduce pollutants that have negative consequences on both humans and the environment. In order to reduce the harmful species the catalytic converter contains noble metals that promote reactions to take place. These reactions are necessary for the reduction of the dangerous species in the exhaust gas.

### 3.1 Combustion Engines and Emissions

A combustion engine takes air and fuel as input and produces power and emissions. The fuel is based on hydrocarbons ( $C_\alpha H_\beta$ ). A schematic picture of a combustion engine can be found in figure 3.1. When the engine is running stoichiometrically ( $\lambda = 1$ ) the fuel and oxygen in the air are in perfect proportion to each other and theoretically the emissions consists only of carbon dioxide, water vapor and nitrogen, see (3.1).



In reality though, small amounts of CO, HC and  $NO_x$  are produced as well, due to non ideal burning in the cylinders. These species are

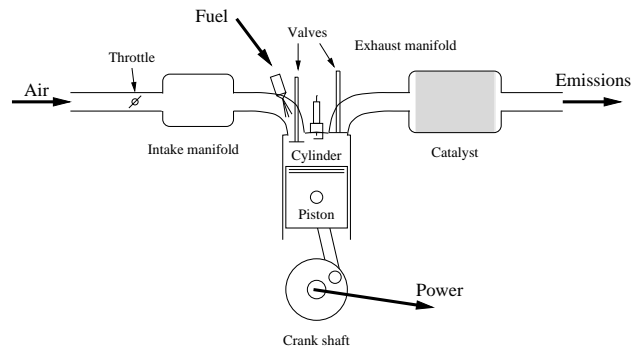


Figure 3.1: Schematic picture of an engine. The engine takes air and fuel as input and generates power and emissions. The picture is taken from [10] and used with permission from the authors.

dangerous to both humans and nature and it is important that they are being reduced as much as possible.

If the engine is running lean there is excess oxygen in the air/fuel mixture. The excess oxygen reacts with nitrogen when the gases are heated in the cylinder and oxides of nitrogen are produced. If the engine is running rich the air/fuel mixture consists of a higher rate of fuel as compared to when the engine runs stoichiometric. Hence the combustion is incomplete and produces carbon monoxide and hydrocarbons.

The least amount of pollutants after the catalytic converter is obtained when the engine is run stoichiometric, see figure 3.2.

## 3.2 The Catalytic Converter

When having a catalytic converter the engine can be allowed to differ from the stoichiometric point for short periods of time, due to the properties of the converter. Simplified, the converter can be compared to a box containing stored oxygen. When the engine runs lean the box is filled with the excess oxygen and when the engine runs rich the oxygen in the TWC is used to oxidize CO and HC. This means that when the box is full the  $\text{NO}_x$  and excess oxygen will pass right through the TWC. When the box is empty the same thing goes for CO and HC. It is therefore desirable to know the relative oxygen level in order to be able to control the lambda value to get a more efficiently run engine. The storage capacity describes the maximum amount of oxygen that is possible to store in the converter.

Most catalytic converters have a honeycomb structure, the wash-

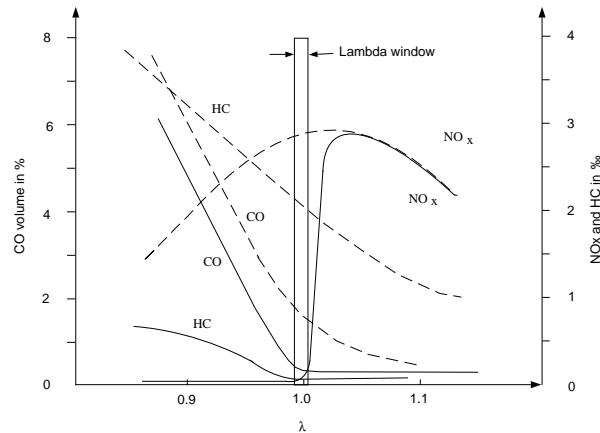


Figure 3.2: Picture of the lambda window, which shows the interval in which acceptable pollution are obtained. Dashed - Before catalyst, Stroked - After catalyst. The picture is taken from [10] and used with permission of the authors.

coat, covered with rhodium, platinum and/or palladium. The washcoat is made of a heat transferring solid phase e.g alumina. The alumina is surface treated with porous materials e.g ceria and zirconium. Figure 3.3 is a schematic view of the structure of a catalytic converter. The role of ceria and ceria based materials in a catalytic converter is to help maintaining the conversion efficiency of the converter. Ceria has the ability to store excess oxygen during lean period and release it during rich conditions to oxidize CO and hydrocarbons.

Since the noble species are expensive and important to the functionality of the converter, it is desirable to have as much surface area exposed to the exhaust stream as possible, while minimizing the amount of noble material. During rich conditions the noble materials promote the conversion of CO and HC. The CO and HC react with stored oxygen, becoming CO<sub>2</sub> and water vapor. During lean conditions the NO<sub>x</sub> gases leave O on the converter when being converted into N<sub>2</sub>.

In order for the converter to work efficiently it must have reached a high temperature, around 450-600 K. The temperature when the conversion reaches 50 % is called light-off temperature. Since most of the polluting is taking place before the light-off temperature is reached, it is important to get a fast heating of the converter. This can be done by putting the converter closer to the engine, but if the converter is too close to the engine the noble materials can be damaged. Another way to reach the light-off temperature early is to pre-heat it using the

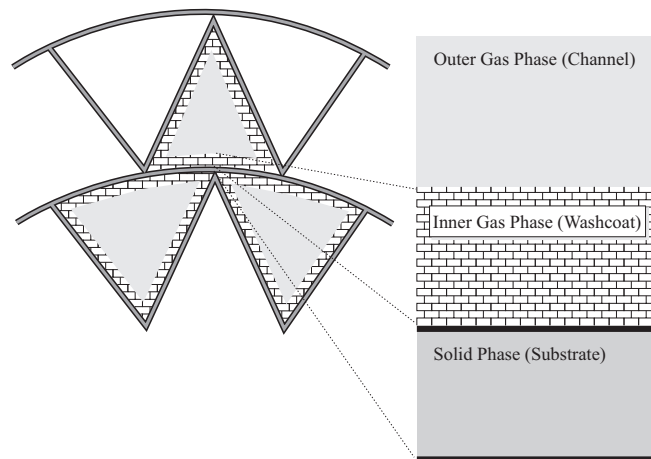


Figure 3.3: Schematic figure of a catalytic converter. The picture is a simplified version of a picture taken from [3] and used with permission of the author.

electrical system of the car. Unfortunately, with the 12 Volt-system used in most cars today it takes several minutes to heat the converter and a majority of people do not wait that long before starting their car.

### 3.3 Study of the dynamics

One way to examine the dynamics of the catalytic converter is to monitor the AFR before the catalytic converter to switch from lean to rich, then back again, and watch the behavior of  $\lambda$  after the catalytic converter as shown in figure 3.4.

For further reading about the dynamics of the converter, [3], [4], [7] and [9] are recommended.

#### 3.3.1 The sensors' influence on the measurements

The sensors have not been widely investigated in this thesis, but since their influence on the measured value is important if the right conclusions are to be drawn, a short introduction is given here.

The sensors are not only sensitive to the  $\lambda$ -value, but also to the gas composition, especially hydrogen has a large effect [11]. This is not a problem before the catalytic converter, since the exhaust gas composition from the engine remains roughly constant for a specific  $\lambda$ -value, and the sensor is calibrated with representative engine-out

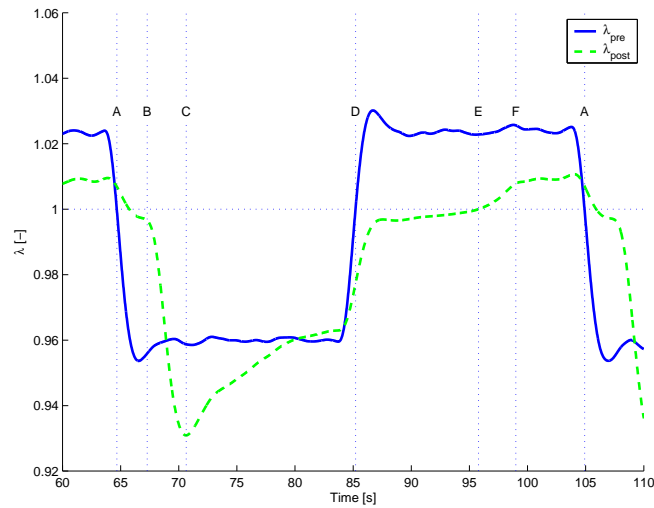


Figure 3.4: Filtered measurements from two wide-range  $\lambda$ -sensors. One sensor is placed before and the other one is placed after the TWC.

exhaust.

Downstream of the catalytic converter however, the gas composition changes dynamically due to the reactions taking place in the converter. The sensor can hence not be well calibrated, and a time-varying bias occurs. Additionally the generation of hydrogen in the TWC changes as the converter ages and hence the biases changes over the converter's lifetime.

Further information about the effect on the sensors can be found e.g. in [3] and [7]. The first also contains information concerning the gas composition downstream of the converter.

### Wide-range versus switch-type sensors after the TWC

In figure 3.4 both the  $\lambda$ -value before the catalytic converter, and the one after the converter have been measured with wide-range  $\lambda$ -sensors in order to make the comparison easier.

Although both wide-range and switch-type  $\lambda$ -sensors depends on the gas composition. A switch-type  $\lambda$ -sensor is often preferred in practice downstream of the converter, due to a number of reasons:

- the switch-type  $\lambda$ -sensor is very precise around the stoichiometric point, even when placed downstream of the TWC. It is thus possible to decide if the  $\lambda$ -value is rich or lean.
- a wide-range  $\lambda$ -sensors suffers from considerable offsets, depend-

ing on the ageing level of the converter and the sensor

- a switch-type  $\lambda$ -sensor is cheaper than a wide-range. Additionally a switch-type  $\lambda$ -sensor is already in use for diagnostic purposes in modern cars, therefore no extra sensor is needed.

### 3.3.2 Study of the measurements

To make the references shorter in this section all capital letters in brackets should be interpreted as references to the corresponding time stamps in figure 3.4.

Both the  $\lambda$ -values before and after the catalytic converter, have been measured with wide-range  $\lambda$ -sensors. It should be noted however, that the characteristics of the sensors are different, and tests have shown that there are offset and gain differences between them even when placed on the same side of the converter.

Before the point where the wide-range  $\lambda$ -sensor before the converter,  $\lambda_{pre}$ , switches from lean to rich (A) the engine has been running lean for quite a while and thus the amount of stored oxygen in the catalytic converter is high and the degree of catalyst deactivation is low. The differences in  $\lambda_{pre}$  and the wide-range  $\lambda$ -sensor after the converter,  $\lambda_{post}$ , should not be paid too much attention because of the difference between the sensors and the influence of the change in gas composition.

Directly after  $\lambda_{pre}$  switches from lean to rich (between A and B)  $\lambda_{post}$  stays close to the stoichiometric level even though  $\lambda_{pre}$  is rich. This is because of the large amount of excess oxygen in the catalytic converter that compensates for the lack of oxygen in the incoming gas.  $\lambda_{post}$  does not start to fall until the converter is out of excess oxygen (B). Then  $\lambda_{post}$  drops to its richest value (C).

During the interval between (B) and (C) the oxygen storage level decreases even more to compensate for the lack of oxygen in the incoming gas. At the same time, the degree of catalyst deactivation is slightly increased due to the rich incoming gas that cannot be oxidized due to the lack of excess oxygen. Hence, the engine is running rich and there is a high amount of vacant sites on the converter's surface, which promotes the hydrogen generating reactions listed in appendix A. The increasing amount of hydrogen makes the  $\lambda_{post}$ -sensor show a richer value than the true one. This explains the big difference between  $\lambda_{post}$  and  $\lambda_{pre}$  at (C).

In the interval between (C) and (D) where both  $\lambda_{pre}$  and  $\lambda_{post}$  show rich values, the degree of catalyst deactivation is continuously increased since there are more species that needs to be oxidized than available oxygen. Hence, the number of vacant sites is decreased, and the hydrogen generation is inhibited. This affects the  $\lambda_{post}$ -sensor, which shows an increasingly leaner value.

When  $\lambda_{pre}$  switches back to lean (D),  $\lambda_{post}$  stays close to the stoichiometric level in the same way as when  $\lambda_{pre}$  switched to rich. At first, the excess oxygen in the incoming gas works to oxidize the species that have been gathered in the catalytic converter during the rich period and caused the catalyst deactivation. Then the excess oxygen in the incoming gas is adsorbed in the converter and increases the level of stored oxygen again.

$\lambda_{post}$  starts to increase when the catalytic converter is close to full with oxygen (E) and reaches its leanest level (F) then stays at the lean level until  $\lambda_{pre}$  switches from lean to rich (A) and everything starts over again.

The reason why the interval between (D) and (E) is much further in time than the interval between (A) and (B) is probably mostly due to biases in the system. Even though the response time when the  $\lambda$  is switched between rich and lean might differ from the response time when it switches from lean to rich.

Both the  $\lambda$ -value measured by the control system, as well as the  $\lambda$ -sensors may suffer from biases. The control system is operated to switch the  $\lambda$ -value between 0.97 and 1.03 but as can be seen in figure 3.4 the measured  $\lambda_{pre}$  is lower than that. Hence, it is possible that the engine is running very rich when running rich, but only slightly lean when running lean, which would explain the difference in time to increase/decrease the catalyst deactivation and fill/empty the converter of stored oxygen.



## Chapter 4

# Model A - A Storage Dominated Model with Reversible Catalyst Deactivation

This chapter describes a model presented by James C. Peyton Jones in [6] and [8]. It is empirical and it is assumed that the dynamics of the catalytic converter are dominated by oxygen storage in the converter and reversible catalyst deactivation. These are not assumed to change over the catalytic converter's spatially distributed nature. Hence, there are two state space variables to describe these two phenomena. This is based on the observation in [6] that all gas components respond to input changes over a similar time-scale. Which shows that the process is dominated by the relatively slow dynamics of gas storage and release, and that the other kinetics occur over a much shorter, and less significant, time-scale.

### 4.1 Model

The model has one input, the wide-range  $\lambda$ -value before the catalytic converter, and one output, the wide-range  $\lambda$ -value after the converter.

Note that the AFR in this model is expressed in terms of the difference from stoichiometric,  $\Delta\lambda = \lambda - 1$ , instead of the more common  $\lambda$ . This makes it possible to model the states of the catalytic converter with a single integrator.

### 4.1.1 The oxygen storage state, $\phi$

The oxygen storage and release rate is dependent on the flow of oxygen into the catalytic converter and the amount of oxygen stored in the converter,  $\phi$ . During lean conditions, when there is an excess of oxygen in the exhaust gas,  $\Delta\lambda_{pre}$  promotes adsorption, and vice versa during rich conditions.

The oxygen storage is described compared to the equilibrium level when the pre-catalyst AFR is stoichiometric, hence  $\phi$  can be both positive and negative. The effect of  $\phi$  on the oxygen storage and release rate is not linear since it becomes increasingly harder to store more oxygen as  $\phi$  increases from zero and vice versa. Hence, a general function,  $N(\phi)$ , with a nonlinear spring characteristic is used. The function  $N(\phi)$  is therefore approximated with a polynomial expansion of  $\phi$ :

$$N(\phi) = a_1\phi + a_2\phi^2 + a_3\phi^3 + a_4\phi^4 + a_5\phi^5,$$

and can be seen in figure 4.1.

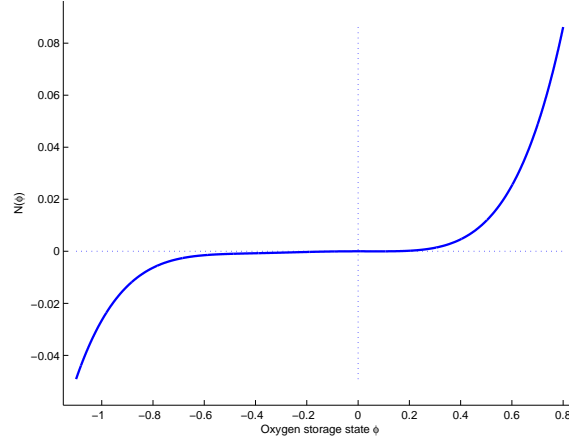


Figure 4.1: The effect of  $\phi$  on the oxygen storage and release rate.

The exception from the above occur during lean to rich transitions when high levels of stored oxygen are available for reducing the rich incoming feed gas (between point A and B in figure 3.4). The oxygen release is then limited only by the feed gas demand.

Hence, it follows that the equation for the oxygen storage rate can be described as:

$$\dot{\phi} = \begin{cases} \dot{m}_f K_\lambda \Delta\lambda_{pre} & (\Delta\lambda_{pre} < 0) \text{ and } (\phi > 0) \\ \dot{m}_f K_\lambda (\Delta\lambda_{pre} - N(\phi)) & \text{otherwise,} \end{cases} \quad (4.1)$$

where  $\dot{m}_f$  is the fuel mass flow to the engine.

### 4.1.2 The reversible catalyst deactivation, $\psi$

The deactivated fraction of the catalytic converter surface increases when there is a deficiency of oxygen both before the converter and after, i.e. when there is a deficiency of oxygen in the incoming feed gas and not enough oxygen stored in the converter to compensate for this (between point B and D in figure 3.4). The rate at which the deactivation increases is proportional to the mass flow into the converter, the lack of oxygen after the catalytic converter,  $-\Delta\Lambda_{post}$ , and the fraction of the surface already occupied by deactivation agents,  $\psi$ . The presence of excess oxygen in the feed gas,  $\Delta\lambda_{pre} > 0$ , on the other hand decreases the deactivation at a rate proportional to the supply of oxygen in the feed gas, until there are no more deactivation agents left on the surface,  $\psi = 0$ , (just after point D in figure 3.4).

The deactivated fraction of the catalytic converter surface,  $\psi$ , can hence be described as follows:

$$\dot{\psi} = \begin{cases} \dot{m}_f K_d (\Delta\Lambda_{post} - \psi) & (\Delta\lambda_{pre} < 0) \text{ and } (\Delta\Lambda_{post} < 0) \\ -\dot{m}_f K_r \Delta\lambda_{pre} & (\Delta\lambda_{pre} > 0) \text{ and } (\psi > 0) \\ 0 & \text{otherwise.} \end{cases} \quad (4.2)$$

Note that  $\Delta\Lambda_{post}$  is the post-catalyst AFR deviation from stoichiometric before the effect of the catalyst deactivation has been taken into account, and thus not equal to  $\Delta\lambda_{post}$ , which is the  $\Delta\lambda$ -value after the catalytic converter.

### 4.1.3 Estimated $\Delta\lambda$ value after the catalytic converter

The  $\Delta\lambda$  value after the catalytic converter depends on the  $\Delta\lambda$  value before the converter, the rate at which oxygen is released compared to the fuel mass flow, and the deactivated fraction of the converter.

$$\begin{aligned} \Delta\lambda_{post} &= \Delta\lambda_{pre} - \frac{1}{\dot{m}_f K_\lambda} \dot{\phi} + K_\psi \psi \\ &= \begin{cases} K_\psi \psi & (\Delta\lambda_{pre} < 0) \text{ and } (\phi > 0) \\ N(\phi) + K_\psi \psi & \text{otherwise} \end{cases} \end{aligned} \quad (4.3)$$

The received output from this model is thus a  $\lambda$ -value that can be compared to the output from a wide-range  $\lambda$ -sensor.

## 4.2 Convert to switch type $\lambda$ -values

To be able to use the wide-range  $\lambda$ -value obtained from the model for control purposes, a reliable wide-range  $\lambda$ -sensor after the catalytic converter is needed. In the articles [6] and [8], the measured values

agree well with the values achieved with the model. The oxygen storage state describes the dynamics of the oxygen filling and depleting, and the distortion of the  $\lambda$ -sensor is taken into account by the reversible catalyst deactivation state. The wide-range  $\lambda$ -sensor used after the converter in this thesis however, suffers from biases and attempts to adapt the model to measured data failed.

One way to solve this problem is to make a model, which converts the wide-range  $\lambda$ -value to a corresponding switch-type  $\lambda$ -value. Since the main concern in this thesis is on the model of the catalytic converter and not on the sensors, a simple solution is to merge the exhaust gas and the sensor models from [3], described in chapter 6, to achieve this  $\lambda$  converter. The augmented model can be seen in figure 4.2.

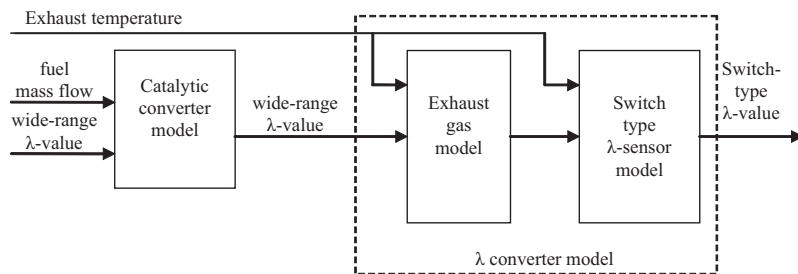


Figure 4.2: Block diagram of the catalytic converter model and the  $\lambda$  converter.

To be able to do this however, several more assumptions and simplifications are needed. First of all the exhaust gas model is developed to be in front of the catalytic converter, i.e. the input signal is supposed to be the  $\lambda$ -value of the gases from the engine. In this case however, the  $\lambda$  after the converter would be used as input.

Secondly, the temperature after the converter is estimated in the converter model in chapter 6, presented in [3], and used as input to the sensor model. With this TWC model, the temperature after the converter is not obtained and hence the assumption that the temperature after the converter is equal to the one before the converter is made.

### 4.3 Parameter Estimation

As described in section 3.3, a wide-range  $\lambda$ -sensor often suffers from biases. Hence, the value measured with the wide-range  $\lambda$ -sensor before the converter is adjusted with an offset to compensate for this.

The parameter estimation was done by simulating the entire model with the four different estimation data described in chapter 2 and min-

imizing the sum of the square error. This can be done according to the scheme below:

- Use the function `fminsearch` in Matlab Optimization Toolbox in order to estimate the parameters in the catalytic converter model. The first time this is done, the start values of the parameters in the exhaust gas and sensor models can be set to the values obtained in chapter 6.
- Use the function `fminsearch` in order to estimate the parameters in the exhaust gas model.
- Once again, use the function `fminsearch` and estimate the parameters in the sensor model.
- Depending on the accuracy of the start values, the previous three steps might have to be repeated. When reasonable values have been obtained, the function `lsqnonlin` in Matlab Optimization Toolbox can be used to estimate all of the parameters, to finally tune them.

The resulting parameter values can be found in appendix B.

Since the model is highly nonlinear it is hard to find the parameters that are optimal in a global sense, and a large number of optimization steps might have to be made to obtain good estimations of the parameters.

### 4.3.1 Catalytic Converter Parameters

The parameters that need to be estimated in this model of the catalytic converter are:

$\mathbf{K}_\lambda$  , a constant of proportionality, which affects the rate at which the oxygen storage state changes.

$\mathbf{K}_d$  , the deactivation constant of proportionality, i.e. it affects the rate at which the deactivation increases.

$\mathbf{K}_r$  , the reactivation constant of proportionality, i.e. it affects the rate at which the deactivation decreases.

$\mathbf{K}_\psi$  , a constant of proportionality, which represents the effect the reversible catalyst deactivation has on the  $\lambda_{post}$ -value.

$a_1 \dots a_5$  , the coefficients in the polynomial describing  $N(\phi)$ .

### 4.3.2 Exhaust Gas and Sensor Parameters

The parameters in the exhaust gas and sensor models are estimated in order to adjust the models to the new conditions, i.e. that the exhaust gas model is placed behind the model of the catalytic converter instead of in front, and the temperature used as input to the sensor model is the one of the exhaust gases instead of the temperature of the gases after the converter.

The parameters to be estimated in the exhaust gas model are:

$$a_{\eta_{comb}}, b_{\eta_{comb}}, \text{ and } \phi_{H_2/CO},$$

and the ones in the sensor model are:

$$A_{\lambda st}, B_{\lambda st}, C_{\lambda st}, D_{\lambda st}, E_{A,\lambda st}, E_{E,\lambda st}, \text{ and } F_{\lambda st}.$$

### 4.3.3 Parameters adjusted to the age of the converter

The catalytic converter's behavior changes as a result of the ageing of the converter. Hence, some parameter values are adjusted over time to account for this. According to [12] it is the converter's storage capacity that is affected. Thus, the parameters that need to be adjusted are the ones, which affect mainly the increase of the oxygen storage rate and the increase of the catalyst deactivation.

The oxygen storage rate depend on the parameter  $K_\lambda$  and the coefficients in the polynomial  $N(\phi)$ , i.e.  $a_1$  to  $a_5$ . Since  $K_\lambda$  is the only parameter that affects the decrease during lean to rich transitions when high levels of stored oxygen are available, and this rate should be significantly the same over time,  $K_\lambda$  is not adjusted. Hence, the parameters that do need to be adjusted are the coefficients  $a_1$  to  $a_5$ .

The catalyst deactivation rate depend on the parameter  $K_d$  when it is increasing and  $K_r$  when it is decreasing. Therefore, it is the parameter  $K_d$  that should be adjusted.

The only remaining parameter in the converter model not considered is  $K_\psi$ . This represents the effect the reversible catalyst deactivation has on the  $\lambda_{post}$ -value and should not be significantly dependent on the converters age.

To sum up, the parameter  $K_d$  and the coefficients  $a_1$  to  $a_5$  should be adjusted as the converter is ageing.

## 4.4 Discussion

The model of the catalytic converter and the merged  $\lambda$  converter are evaluated in order to see if they together make a good estimation of the

switch-type  $\lambda$ -value after the converter, and if the states act the way they are expected to.

#### 4.4.1 The extension to switch-type $\lambda$ -values

As mentioned earlier two large simplifications were made to be able to merge the exhaust gas model and the sensor model in chapter 6, presented in [3], into a  $\lambda$  converter.

The first one was that the exhaust gas model could be used after the catalytic converter, instead of before the converter. The composition of the gases for a specific  $\lambda$ -value before the converter is roughly constant, as described in section 3.3. This knowledge is used when the concentrations are calculated in the exhaust gas model. The gas composition downstream of the converter however, changes dynamically (also this is described in section 3.3). This model should thus not be expected to produce the correct concentrations at e.g. different operating points.

The second simplification was to use the exhaust gas temperature before the converter instead of the one after the TWC as input to the exhaust gas and the sensor model. In reality, the behavior of the exhaust gas temperature before and after the converter is very different. When the engine is running rich, the exhaust gas temperature is low. This leads to a high amount of unburned fuel that instead reaches the converter and makes the temperature rise in the gases that leaves the TWC. Hence, in this case, low exhaust gas temperatures lead to higher temperatures of the gases after the converter.

In order to make the exhaust gas and sensor models as accurate as possible under these new conditions, the parameters in the models were estimated in this chapter as well. However, it should be noted that the resulting  $\lambda$  converter not is expected to be very reliable. A benefit from using it though, is that a switch-type  $\lambda$ -sensor can be used downstream of the converter, instead of a wide-range. As described in section 3.3, a switch-type sensor is often preferred.

#### Parameter values in the exhaust gas and sensor models

The adjustments made in the parameters can be seen when comparing the values of the parameters obtained in this chapter, which can be found in appendix B, with the values estimated in 6, found in appendix C.

In the exhaust gas model, the coefficients relating to the temperature,  $a_{\eta_{comb}}$  and  $b_{\eta_{comb}}$ , has changed the sign. Additionally a big increase in  $\phi_{H_2/CO}$  can be seen, which suggests that there are a lot more hydrogen as compared to CO in the gas after the converter than before, as expected.

In the sensor model's parameters the major differences can be found in the parameters  $B_{\lambda st}$ ,  $C_{\lambda st}$ ,  $D_{\lambda st}$  and  $E_{E, \lambda st}$ . The first three is directly connected to the concentrations, i.e. the output from the exhaust gas model, and the fourth to the temperature.

#### 4.4.2 Validation

The model is validated with the validation data described in chapter 2. The switch-type  $\lambda$ -values estimated by the model, as well as the measured values can be seen in figure 4.3. The corresponding oxygen storage state and the reversible catalyst deactivations can be seen in figure 4.4 and 4.5.

As mentioned earlier, the gas composition after the converter is dependent on the operating point but the  $\lambda$  converter is not able to catch this behavior. Hence, the model is adapted to make the errors for the four data sets as small as possible. Since there are two sets of data for operating point number 2, as described in chapter 2, and this operating point additionally is between operating point number 1 and 3, the model is hence primarily calibrated to match the data from operating point number 2. The second and third simulation are hence the ones least affected by the errors of the  $\lambda$  converter, and therefore the ones of highest interest when the model of the catalytic converter is to be examined.

##### The switch-type $\lambda$ -sensor value

As can be seen in figure 4.3 the model is good at predicting the switch-type  $\lambda$ -value after the catalytic converter in the second and third simulation. The richest and leanest levels estimated by the model are close to the levels measured, and the points at which  $\lambda$  switches from lean to rich and vice versa is close to the measured ones. The agreement in the first and fourth simulation is less accurate. It is hard to tell whether this is solely due to less accuracy in the  $\lambda$ -converter model, or not.

At the end of the plot, when the  $\lambda$ -value before the catalytic converter switches fast between lean and rich, the estimated switch-type  $\lambda$ -value slowly converges with the measured in the second and third simulation.

##### The oxygen storage state

The accuracy of the estimations of the oxygen storage level is harder to determine. Although it seems reasonable with a high value after the engine has been running lean, and a low value when running rich.

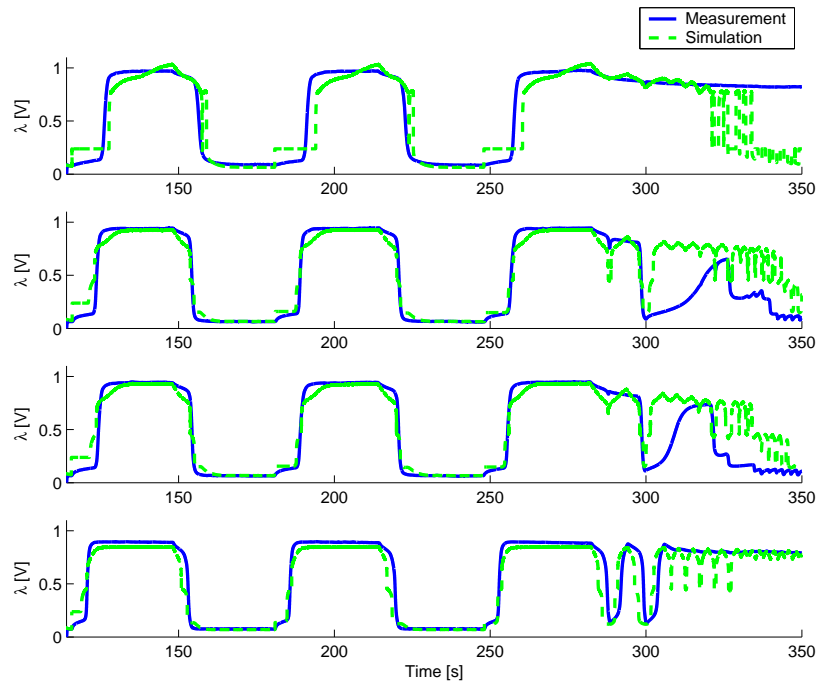


Figure 4.3: The filtered measured and simulated switch-type  $\lambda$ -values from the four operating points (see 2.2).

### The deactivation state

Since the hydrogen generation is closely connected to the deactivation level, the weakness of the  $\lambda$  converter affects the accuracy of the deactivation state. One should hence not attach to much attention to the deactivation state estimated by the model. However, it can be noted that it seems to increase when the engine is running rich, and decrease when running lean, as expected. A drawback is that its value does not decrease to zero as the engine runs rich.

Even though the reversible catalyst deactivation is not paid much attention, it should be noted that errors in this state affect the  $\lambda$ -value and the oxygen storage state as well.

### 4.4.3 Results

Without a  $\lambda$  converter with high accuracy, or a wide-range  $\lambda$ -sensor without biases after the TWC, it is hard to evaluate the model of the catalytic converter. Even though it captures the dynamics of the converter well for some of the measurements in this thesis, it is not assumed

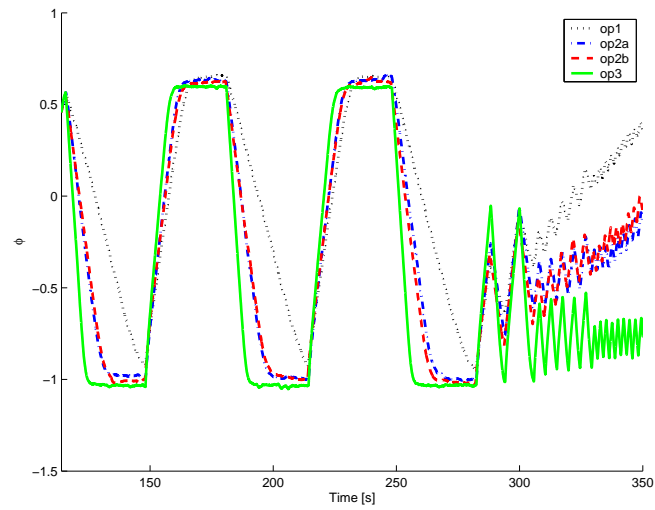


Figure 4.4: The estimated oxygen storage level for the four data sets.

to do this regardless of the operating point or the age of the converter. Additionally, even if the model of the converter is very accurate it cannot be used in an engine control system without a sufficient  $\lambda$  converter model.

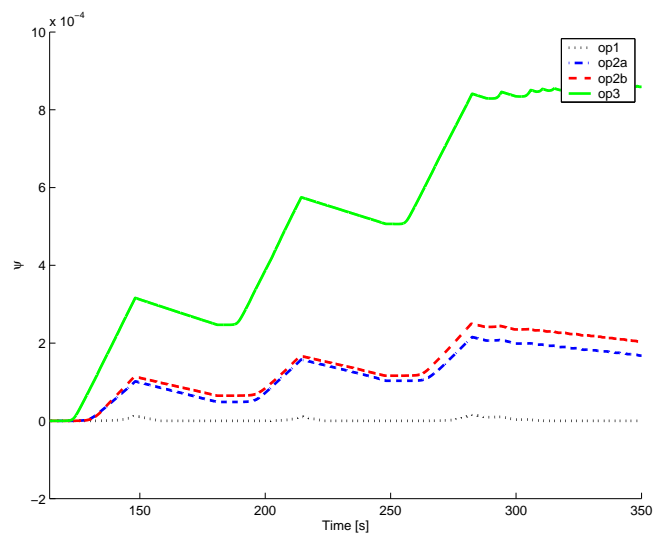


Figure 4.5: The estimated reversible deactivation fraction for the four data sets.



## Chapter 5

# Model B - A Model Consisting of One Nonlinear Integrator

This model is presented by Mario Balenovic in [4]. The model is basically a nonlinear integrator with one state representing oxygen coverage, one parameter which gives an indication on the converters' storage capacity and a function that represents the relative conversion. The model has one input and one output, the wide-range  $\lambda$ -sensor signals before and after the catalytic converter, respectively.

### 5.1 Model

The model is developed in order to control the engine based on the state of the catalytic converter. In this case the desired controlled variable is the degree of ceria coverage by oxygen containing species (relative oxygen coverage of ceria, ROC).

#### 5.1.1 Model development

Model assumptions:

- The dynamic behavior of the catalytic converter is only due to the oxygen storage and release capabilities of ceria.
- Reactions taking place on the noble metal surface are assumed to be instantaneous.
- The oxygen storage filling can be represented by a single variable.

- Both the lambda sensors (before and after the catalytic converter) are ideal
- CO is not taken into account when calculating the relative oxygen coverage of ceria.

It is also assumed that there are only CO and O<sub>2</sub> in the exhausts and that the converters' length is almost zero. These assumptions make it possible to model only one point in the converter. The species can react in the converter either by surface reactions or by oxidation or reduction on the ceria. The outgoing concentration of CO is the incoming concentration of CO minus the CO that reacts on the surface and the CO that reacts with ceria. The same goes for O<sub>2</sub>. The surface reactions are assumed to be immediate. This means that the incoming CO or O<sub>2</sub> and the CO or O<sub>2</sub> that is left after the reaction with the surface can be called the excess of the species. Then the outlet concentrations for rich inlet feed can be written as following:

$$\begin{aligned} c_{COout} &= c_{COex} - r_{CO} \\ c_{O_2out} &= 0 \end{aligned} \quad (5.1)$$

and for lean inlet feed:

$$\begin{aligned} c_{COout} &= 0 \\ c_{O_2out} &= c_{O_2ex} - r_{O_2} \end{aligned} \quad (5.2)$$

The subscript *ex* denotes the excess of the species after a surface reaction has been completed and *r* is the reaction rate on the ceria.

During lean conditions the disappearance rate of excess O<sub>2</sub> is proportional to the oxygen storage filling:

$$r_{O_2} \sim \frac{d\xi}{dt} = \frac{1}{L} k_{fill} c_{O_2} (1 - \xi). \quad (5.3)$$

Correspondingly the disappearance rate of excess CO during rich conditions is proportional to the oxygen storage emptying:

$$r_{CO} \sim -\frac{d\xi}{dt} = -\frac{1}{L} k_{emp} c_{CO} \theta_{CO} \xi, \quad (5.4)$$

where  $\xi$  is the local fraction of oxygen storage. These equations are based on equations from a more advanced model, also presented in [4].

The  $\lambda$  value can be expressed in terms of oxidants (O), reactants (R) and products (P):

$$\lambda = \frac{O + P}{R + P}, \quad P \gg O, P \gg R. \quad (5.5)$$

It will be assumed that all oxidants can oxidize ceria and all reactants can reduce ceria. Only the excess of reactants or oxidants will be needed for the model input, hence the following holds:

$$\begin{aligned}\lambda_{lean} &\approx \frac{O_{ex}}{P} + 1 \\ \lambda_{rich} &\approx 1 - \frac{R_{ex}}{P}.\end{aligned}\tag{5.6}$$

In order to get the  $\lambda_{rich}$  equation a first order Taylor series has been used. This holds as long as the input does not become very rich. Since only the excess of reactants or oxidants will be needed for model input the lambda excess,  $\lambda - 1$ , will be used. The lambda excess will be denoted  $\Delta\lambda$ . Taking into account (5.1) and (5.2) the final model (for one point of the converter) that holds in both lean and rich regions becomes:

$$\Delta\lambda_{out} = \Delta\lambda_{in} - k_d \frac{d\xi}{dt}.\tag{5.7}$$

Replacing the local variable  $\xi$  with  $\zeta$  representing the relative oxygen coverage of ceria for the whole reactor, this model is valid also for the whole converter. Since the complete reactor is modeled as a series of almost zero-length reactors the expressions (5.3) and (5.4) has to be modified. Since they become nonlinear when more than one reactor is connected in series an alternative approach has to be taken. The global reaction rate can therefore be expressed as:

$$\frac{d\zeta}{dt} = k_{gr} \Delta\lambda_{in} f(\zeta).\tag{5.8}$$

$k_{gr}$  is a scaling factor and the function  $f(\zeta)$  is a nonlinear function depending on the inlet feed.  $f(\zeta)$  is in fact two functions,  $f_L$  for lean input and  $f_R$  for rich input. If (5.7) and (5.8) are put together the expression for  $\Delta\lambda$  becomes:

$$\Delta\lambda_{out} = \Delta\lambda_{in} (1 - k_d k_{gr} f(\zeta))\tag{5.9}$$

Under the assumption that the outlet lambda cannot have the opposite sign of the inlet lambda,  $(1 - k_d k_{gr} f(\zeta))$  cannot be below 0 or exceed 1. This means that  $k_d k_{gr} f(\zeta)$  also is bounded in the same interval. Since the function  $f$  has to be estimated the two scaling factors can be included in  $f$ . It will also be assumed that  $k_{gr} = \frac{1}{k_d}$ . Thus, the model becomes:

$$\frac{d\zeta}{dt} = \frac{1}{k_d} \Delta\lambda_{in} f(\zeta)\tag{5.10}$$

$$\Delta\lambda_{out} = \Delta\lambda_{in} - k_d \frac{d\zeta}{dt}\tag{5.11}$$

$$= \Delta\lambda_{in} (1 - f(\zeta)).\tag{5.12}$$

### 5.1.2 The complete model

The assumption that the inlet and outlet lambda value cannot have opposite signs is not always true. During a rich-to-lean step the outlet stays rich for a short period of time even though the inlet is lean, see [4]. This can also be seen after point D in figure 3.4. This is due to CO and HC desorption from the ceria surface and the noble metal surface. The model (5.10) cannot describe this, thus some modification should be made. One way of solving this is to add an additional function to account for the desorption effect. The final model becomes:

$$\frac{d\zeta}{dt} = \frac{1}{k_d}(\Delta\lambda_{in}f(\zeta) + g(\zeta)) \quad (5.13)$$

$$\Delta\lambda_{out} = \Delta\lambda_{in} - k_d \frac{d\zeta}{dt} \quad (5.14)$$

$$= \Delta\lambda_{in}(1 - f(\zeta)) + g(\zeta). \quad (5.15)$$

The strictly positive function  $g(\zeta)$  is only activated when the inlet is stoichiometric or lean and thus it is possible to model rich output with lean inputs.

### 5.1.3 Model parameters and functions

The only parameter in the model,  $k_d$ , is the inverse of the integrator gain and gives an indication of the oxygen storage capacity. Since a higher mass flow through the engine will fill up the catalytic converter with oxygen faster than a low mass flow,  $k_d$  is also dependent on the mass flow. As already mentioned, the function  $f$  is in fact two functions,  $f_L$  for lean conditions and  $f_R$  for rich conditions. These functions represent the relative conversion. The typical appearance of the functions is shown in fig 5.1. For lean input the left picture in fig 5.1 is

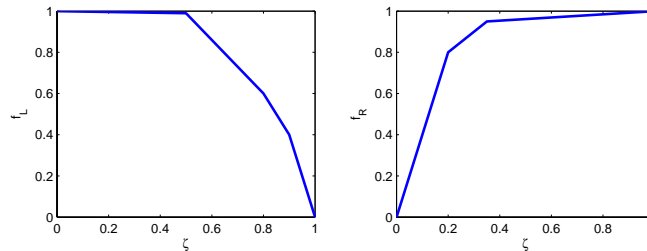


Figure 5.1: A typical appearance of the functions  $f_L$  and  $f_R$ .

the function used. Looking at (5.15) and figure 5.1 it can be seen that when the ROC ( $\zeta$ ) is 1, the  $\lambda$  outlet is equal to the input, assuming that  $g(\zeta) = 0$ . This is reasonable since no more of the excess oxygen can be

stored when  $\zeta = 1$ . The less oxygen stored in the catalytic converter, the closer to 1  $f_L$  gets, which means that  $\Delta\lambda_{out}$  approaches zero, i.e.  $\lambda \approx 1$ . For rich input it is the other way around. When there is a lot of stored oxygen almost all of the reducing species in the converter reacts with the stored oxygen and  $\Delta\lambda_{out}$  is close to zero. When the converter is empty of stored oxygen all the exhaust coming in to the converter also comes out. Both  $f_L$  and  $f_R$  is dependent on the mass flow.

The function  $g(\zeta)$  has been added to the model in order to be able to model rich output with lean input. The function is activated only when the input is stoichiometric or lean and is also dependent on the mass flow.

Since both parameter and functions are dependent on the mass flow, Balenovic made additional changes in the model in order to make the model better in a wider operating range. These changes will not be presented here but can be viewed in [4].

Both parameter and functions are dependent on the mass flow. However, in [4] additional changes in the model is presented, which makes the model better in a wider operating range. These changes will not be presented here.

## 5.2 Parameter estimation

It is desirable to have an easy parameter estimation algorithm which can be used online, since the behavior of the catalytic converter changes over time. The parameter estimation algorithm presented in [4] requires very short testing time. The parameters and functions that need to be estimated are  $k_d$ ,  $f(\zeta)$  and  $g(\zeta)$ .  $k_d$  is very straight-forward to get. From (5.14) it follows:

$$k_d d\zeta = (\Delta\lambda_{in} - \Delta\lambda_{out}) dt. \quad (5.16)$$

If a test begins after the engine has run rich for a while and the oxygen storage is  $\zeta = 0$  and ends after  $T_{ss}$  seconds with a completely filled oxygen storage the following holds:

$$\begin{aligned} k_d &= \frac{\int_0^{T_{ss}} (\Delta\lambda_{in} - \Delta\lambda_{out}) dt}{\int_0^1 d\zeta} \\ &= \int_0^{T_{ss}} (\Delta\lambda_{in} - \Delta\lambda_{out}) dt \end{aligned} \quad (5.17)$$

The same approach can be used when the catalytic converter is initially filled and empty at the end of the test. (5.17) can be approximated with the following sum:

$$k_d = \sum_{k=1}^N (\Delta\lambda_{in}(k) - \Delta\lambda_{out}(k)) T_s, \quad (5.18)$$

where  $N$  is the total number of samples and  $T_s$  is the sampling time.

The same data and the same equation can be used to get  $\zeta(t)$  which can be used to estimate the function  $f(\zeta)$  ( $g(\zeta)$  is neglected here). From (5.15) it follows:

$$f(\zeta) = 1 - \frac{\Delta\lambda_{out}}{\Delta\lambda_{in}}. \quad (5.19)$$

When calculating (5.19) for all samples,  $F(k)$  is obtained. Instead of using a map with  $F(k)$  and  $\zeta(k)$  a simpler function  $\hat{f}(\zeta)$  is calculated with a least squares algorithm.  $\hat{f}(\zeta)$  is approximated by a piecewise linear function. This function can be written as a linear combination of triangular basis functions:

$$\hat{f}(\zeta) = \frac{\sum_{i=1}^n b_i(\zeta) f_i}{\sum_{i=1}^n b_i(\zeta)}, \quad (5.20)$$

where the triangular basis functions are:

$$b_i(\zeta) = \begin{cases} 0, & \text{if } \zeta < \zeta_{i-1}, i \geq 2 \\ \frac{\zeta - \zeta_{i-1}}{\zeta_i - \zeta_{i-1}}, & \text{if } \zeta_{i-1} \leq \zeta < \zeta_i, i \geq 2 \\ 1 - \frac{\zeta - \zeta_i}{\zeta_{i+1} - \zeta_i}, & \text{if } \zeta_i \leq \zeta < \zeta_{i+1}, i \leq n - 1 \\ 0, & \text{if } \zeta \geq \zeta_{i+1}, i \leq n - 1. \end{cases} \quad (5.21)$$

Good results have been obtained in [4] when predefining the basis functions. With fixed basis functions equation (5.20) has an analytical solution. The parameters  $f_{1,2..n}$  are tuning parameters to the  $n$  basis functions. A piecewise linear function with five points should be enough. An example on how to solve the least square problem can be found in [4].

The function  $g(\zeta)$  can be obtained in a similar manner. The data used to estimate the function is taken during a rich to lean step. Since the function only will be used when inlet and outlet lambda have different signs and when  $\Delta\lambda_{in} \geq 0$ , the data set is calculated by:

$$G(k) = \begin{cases} \Delta\lambda_{out}, & \text{if } \Delta\lambda_{out} < 0 \\ 0, & \text{if } \Delta\lambda_{out} \geq 0 \end{cases} \quad (5.22)$$

$$F(k) = \begin{cases} 1, & \text{if } \Delta\lambda_{out} < 0 \\ 1 - \frac{\Delta\lambda_{out}}{\Delta\lambda_{in}}, & \text{if } \Delta\lambda_{out} \geq 0. \end{cases} \quad (5.23)$$

The function  $\hat{g}(\zeta)$  does not have to be as accurate as  $f$ , so a piecewise linear function with two or three point should be sufficient.  $\hat{g}(\zeta)$  can be calculated in the same manner as  $\hat{f}(\zeta)$ .

### 5.3 Validation

During the parameter estimation, the accuracy of the lambda sensor signals is crucial. Neither the pre nor the post catalytic converter sensor

can have any biases. No such lambda sensor signals have been available and therefore the model has not been tested.

The reason why this model is included in this thesis, is that with accurate  $\lambda$ -sensors, the model should give satisfying result. The model is also very simple with only one state and it needs no parameter optimization, only calculations of the parameter and states. Hence, the model should be easy to fit into an engine control system and need little CPU power.



## Chapter 6

# Model C - A Simplified Physical Exhaust Gas Aftertreatment Model

This model has been developed by Theophil Sebastian Auckenthaler and is presented in [3]. The model is a physical model of the exhaust gas aftertreatment system, which includes a reversible wide-range  $\lambda$ -sensor model before the converter, a switch-type  $\lambda$ -sensor model after the converter, and of course a TWC model.

The model is based on reaction kinetics of a small number of key gas components and reactions together with the dynamics of gas storage on the converter surface. The spatially distributed nature of the converter is approximated by a lumped parameter model. The ageing of the TWC is represented by the parameter describing the storage capacity, hence the storage capacity is the only parameter that is assumed to change over time.

### 6.1 Model

The model consists of three modules, see fig 6.1.

The input to the model is the wide-range lambda sensor signal upstream of the TWC, the exhaust mass flow and temperature, and the output is the switch-type lambda sensor signal.

#### 6.1.1 Exhaust gas model

The main purpose of the exhaust gas model is to convert the wide-range lambda sensor value into mole fractions of  $O_2$ ,  $CO$  and  $H_2$ . These mole

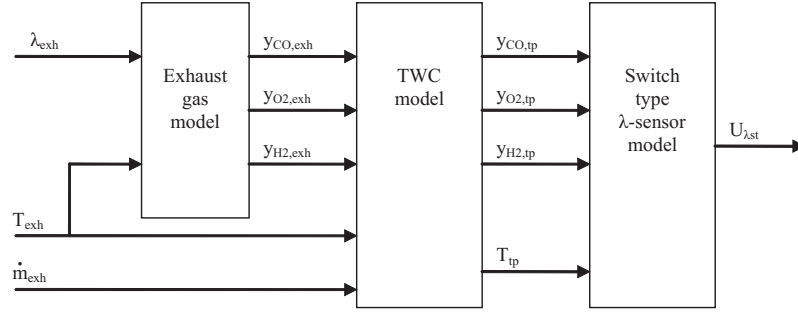
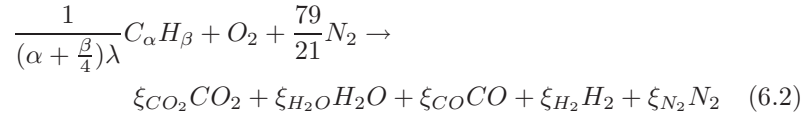
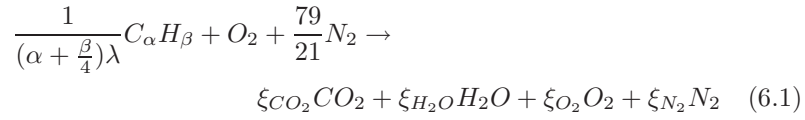


Figure 6.1: Block diagram of the complete model.

fractions are calculated from the combustion reactions when the engine is running lean ( $O_2$  mole fraction) and when the engine is running rich (CO and  $H_2$  mole fractions).



The combustion reactions for lean and rich engine conditions are given in equations (6.1) and (6.2), respectively. Perfect combustion is assumed. The fuel is assumed to be  $C_\alpha H_\beta$ .

During lean conditions all oxidizing components has been collected into  $O_2$ . Hence, the  $O_2$  mole fraction is

$$\begin{aligned} y_{O_2} &= \frac{\xi_{O_2}}{\sum_{i=CO_2, H_2O, O_2, N_2} \xi_i} \\ &= \frac{1 - \frac{1}{\lambda}}{\frac{\alpha + \beta/2}{(\alpha + \beta/4)\lambda} + (1 - \frac{1}{\lambda}) + \frac{79}{21}}. \end{aligned} \quad (6.3)$$

The mole fractions for CO and  $H_2$  can be calculated if the ratio between  $H_2$  and CO ( $\phi_{H_2/CO}$ ) is assumed to be constant. This assumption is motivated in [3].

$$\begin{aligned}
y_{CO} &= \frac{\frac{2}{1+\phi_{H_2/CO}}\left(\frac{1}{\lambda} - 1\right)}{\frac{\alpha+\beta/2}{(\alpha+\beta/4)\lambda} + \frac{79}{21}} \\
y_{H_2} &= \frac{\frac{2\phi_{H_2/CO}}{1+\phi_{H_2/CO}}\left(\frac{1}{\lambda} - 1\right)}{\frac{\alpha+\beta/2}{(\alpha+\beta/4)\lambda} + \frac{79}{21}}.
\end{aligned} \tag{6.4}$$

Since species have been lumped together it is important to remember that the mole fractions contain fractions of other species as well. It has been found that it is critical that the final mole fractions are consistent in terms of the air/fuel ratio  $\lambda$ , but it is not so critical that they are accurate. To make the air/fuel ratio consistent, the author of [3] found a heuristic function:

$$\begin{aligned}
\Delta y_{O_2} &= \frac{\eta_{comb}}{1 + 10|\lambda - 1|} \\
\Delta y_{CO} &= \frac{2}{1 + \phi_{H_2/CO}} \frac{\eta_{comb}}{1 + 10|\lambda - 1|} \\
\Delta y_{H_2} &= \frac{2\phi_{H_2/CO}}{1 + \phi_{H_2/CO}} \frac{\eta_{comb}}{1 + 10|\lambda - 1|}
\end{aligned} \tag{6.5}$$

where

$$\eta_{comb} = a_{\eta_{comb}} + b_{\eta_{comb}} T_{exh}. \tag{6.6}$$

When the efficiency of the combustion increase the temperature of the exhaust gas increase and the concentrations of the reducing and oxidizing species that reaches the catalytic converter decreases.  $\eta_{comb}$  can be interpreted as an inverse combustion efficiency. The factor is dependent on the exhaust gas temperature and has strong impact on the energy balance of the TWC.

The final mole fractions are:

$$y_{i,exh} = y_i + \Delta y_i. \tag{6.7}$$

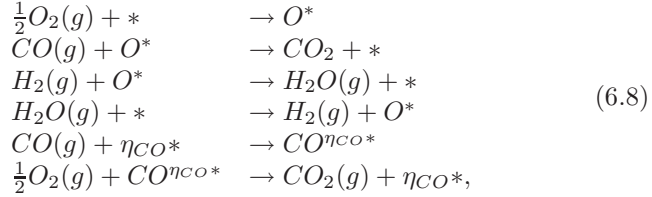
These mole fractions are the input to the TWC-model.

### 6.1.2 TWC model

The TWC model takes the concentrations of the species before the TWC, exhaust gas temperature, and exhaust mass flow as input, and pass on the concentrations of the species after the TWC and the tailpipe temperature to the switch-type  $\lambda$ -sensor.

### Chemical Reactions and Reaction Rates

The number of chemical reactions taking place in a catalytic converter are far too many and complex to be described in detail in this thesis. Extensive information on the chemical reactions taking place in a catalytic converter can be found in [4] and [3]. After extensive assumptions, simplifications, and eliminations done in [3] the following chemical reactions remains:



where \* denotes a vacant site on the catalytic converter surface, and the superscript \* stands for adsorbed species.

The reaction rates depend on the reaction coefficient,  $k_i$ , the concentration of the current species in the washcoat,  $c_i^{wc}$ , and the fraction of the catalytic converter surface that is either vacant,  $\theta_V$ , or occupied by the necessary species,  $\theta_i$ .

Consequently the reaction rates corresponding to the chemical reactions are:

$$\begin{aligned}
 r_{O_2}^{ads} &= k_1 c_{O_2}^{wc} \theta_V \\
 r_{CO}^{red} &= k_2 c_{CO}^{wc} \theta_O \\
 r_{H_2}^{red} &= k_3 c_{H_2}^{wc} \theta_O \\
 r_{H_2O}^{ads} &= k_4 \theta_V^2 \\
 r_{CO}^{ads} &= k_5 c_{CO}^{wc} \theta_V \\
 r_{CO}^{ox} &= k_6 c_{O_2}^{wc} \theta_{CO},
 \end{aligned} \tag{6.9}$$

where the fraction of the catalytic converter surface that is vacant,  $\theta_V = 1 - \theta_O - \theta_{CO}$ . The reaction coefficients are obtained by using the Arrhenius equation, hence  $k_i = A_i e^{\frac{-E_i}{RT_s}}$ ,  $i = 1..6$ .

Since the water concentration is assumed to be constant, it has been included in the pre-exponential factor  $A_4$ , the water adsorption rate is thus independent of this concentration.

### Occupancy of O and CO

The first and fourth chemical reaction increases the fraction of the catalytic converter surface occupied by oxygen, and the fifth reaction increases the fraction of the converter surface occupied by CO but with the higher rate  $\eta_{CO}$ . In a similar way the second, third and sixth

reaction decreases the fraction of the converter surface occupied by the species in question.

The balance equations for the occupancies of O and CO can hence be expressed as follows:

$$\begin{aligned}\frac{\partial\theta_O}{\partial t} &= r_{O_2}^{ads} - r_{CO}^{red} - r_{H_2}^{red} + r_{H_2O}^{ads} \\ \frac{\partial\theta_{CO}}{\partial t} &= \eta_{CO}(r_{CO}^{ads} - r_{CO}^{ox}).\end{aligned}\tag{6.10}$$

### Concentrations

The concentrations are calculated from the set of mass balance equations for the species in the channel,  $c^{ch}$ , and in the washcoat,  $c^{wc}$ . To make a simple model the TWC is discretized along the flow axis into a small number,  $n_c$ , of cells. Then the rate at which the concentration of species  $i$  in the channel changes in cell  $j$ , is assumed to be dependent only of the difference between concentrations in the channel in the previous and the present cell, and the difference between concentrations in the channel and the washcoat in the present cell.

$$\frac{\partial c_{i,j}^{ch}}{\partial t} = f(c_{i,j-1}^{ch} - c_{i,j}^{ch}, c_{i,j}^{ch} - c_{i,j}^{wc})$$

The rate at which the concentration of species  $i$  in the washcoat changes in cell  $j$  is assumed to be dependent only of the difference between concentrations in the channel and the washcoat in the present cell, and the storage capacity,  $SC$ , which is assumed to be constant over the catalytic converter.

$$\frac{\partial c_{i,j}^{wc}}{\partial t} = f(c_{i,j}^{ch} - c_{i,j}^{wc}, SC)$$

Since the dynamics of the gas species are much faster than the ones of the oxygen storage deactivation the mass balance equations can be applied as static equations. From these assumptions, the following terms for both the channel and the washcoat concentrations of  $O_2$ ,  $CO$

and  $H_2$  are obtained:

$$\begin{aligned}
c_{O_2,j}^{ch} &= \frac{\dot{V}_{rel} c_{O_2,j-1}^{ch}}{\dot{V}_{rel} + D_{O_2} \left( 1 - \frac{D_{O_2}}{D_{O_2} + 0.5(k_1\theta_{V,j} + k_6\theta_{CO,j})SC} \right)} \\
c_{CO,j}^{ch} &= \frac{\dot{V}_{rel} c_{CO,j-1}^{ch}}{\dot{V}_{rel} + D_{CO} \left( 1 - \frac{D_{CO}}{D_{CO} + (k_2\theta_{O,j} + k_5\theta_{V,j})SC} \right)} \\
c_{H_2,j}^{ch} &= \frac{\dot{V}_{rel} c_{H_2,j-1}^{ch} + \frac{D_{H_2} k_4 \theta_{V,j}^2 SC}{D_{H_2} + k_3 \theta_{O,j} SC}}{\dot{V}_{rel} + D_{H_2} \left( 1 - \frac{D_{H_2}}{D_{H_2} + k_3 \theta_{O,j} SC} \right)} \\
c_{O_2,j}^{wc} &= \frac{D_{O_2} c_{O_2,j}^{ch}}{D_{O_2} + 0.5(k_1\theta_{V,j} + k_6\theta_{CO,j})SC} \\
c_{CO,j}^{wc} &= \frac{D_{CO} c_{CO,j}^{ch}}{D_{CO} + (k_2\theta_{O,j} + k_5\theta_{V,j})SC} \\
c_{H_2,j}^{wc} &= \frac{D_{H_2} c_{H_2,j}^{ch} + k_4 \theta_{V,j}^2 SC}{D_{H_2} + k_3 \theta_{O,j} SC},
\end{aligned} \tag{6.11}$$

where  $c_{i,j-1}^{ch}$  stands for the concentration of species  $i$  in the preceding cell or at the TWC inlet if  $j = 1$ .  $SC$  is the storage capacity of the TWC.  $D_i = C_i A_{geo}$  where  $C_i$  is the convection mass transfer coefficient of species  $i$ , and  $A_{geo}$  is the specific geometric catalytic converter surface.  $\dot{V}_{rel} = \frac{\dot{V}}{V_{TWC}/n_c}$  where  $\dot{V}$  is the volumetric flow of the exhaust gas,  $V_{TWC}$  denotes the total volume of the TWC, and  $n_c$  is the number of cells.

The channel concentrations of the last cell are the actual output variables, which are fed into the switch-type  $\lambda$ -sensor model.

### Temperature

The temperatures are calculated from the set of energy balance equations for the solid and the gas phase. The rate at which the gas phase temperature,  $T_g$ , changes is assumed to be dependent only of the derivative of the gas phase temperature along the axial position,  $\frac{\partial T_g}{\partial z}$ , and the difference between the solid phase and the gas phase temperature,  $T_s - T_g$ . Since the dynamics of the exhaust gas temperature, are expected to be much faster than the one of the solid temperature, the dynamics of the exhaust gas temperature are neglected. Hence, the following equation for the exhaust gas temperature of cell  $j$  is obtained:

$$T_{g,j} = \frac{\frac{\dot{m}}{V_{TWC}/n_c} c_{p,g} T_{g,j-1} + \alpha A_{geo} T_{s,j}}{\frac{\dot{m}}{V_{TWC}/n_c} c_{p,g} + \alpha A_{geo}}, \tag{6.12}$$

where  $V_{TWC}/n_c$  is the volume of one cell.  $T_{g,j-1}$  is the gas temperature of the preceding cell, except for the first cell where  $T_{g,j-1}$  denotes the inlet gas temperature.

The rate at which the solid phase temperature changes is assumed to be dependent only of the second derivative of the solid phase temperature along the axial position,  $\frac{\partial^2 T_s}{\partial z^2}$ , the difference between the solid phase and the gas phase temperature, the reaction enthalpies, and the difference between the solid phase and the ambient temperature. The second derivative of the temperature has to be discretized, which is done with a backward difference scheme. Since the CO and the H<sub>2</sub> oxidation are the only global oxidation reactions occurring it is assumed that the only enthalpies needed is  $\Delta H_{CO_2}$  and  $\Delta H_{H_2O}$ , even though NO and HC are included in the O<sub>2</sub> and CO concentrations.

Solid phase temperature in cell j  $T_{s,j}$ :

$$\begin{aligned} \frac{\partial T_{s,j}}{\partial t} = & \frac{(1-\varepsilon)\lambda_s \frac{T_{s,j-1} - 2T_{s,j} + T_{s,j+1}}{dz^2} - \alpha A_{geo}(T_{s,j} - T_{g,j})}{\rho_s c_s (1-\varepsilon)} \\ & + \frac{SC((-r_2 - r_6)\Delta H_{CO_2} + (-r_3 + r_4)\Delta H_{H_2O})}{\rho_s c_s (1-\varepsilon)} \\ & - \frac{\alpha_{cat}(T_{s,j} - T_{amb}) \frac{4}{D_{TWC}}}{\rho_s c_s (1-\varepsilon)}, \end{aligned} \quad (6.13)$$

where  $\alpha_{TWC}$  is the heat transfer coefficient from the TWC to the ambient air.  $A_{TWC}$  is the outer TWC surface and  $D_{TWC}$  is the TWC's diameter.

### 6.1.3 Switch-type $\lambda$ -sensor model

It has been shown (see [11]) that it is not only oxygen that affect the tailpipe  $\lambda$ -sensor, H<sub>2</sub> and other reducing species has strong impact on the sensor output, especially during rich conditions. Therefore the reducing species as well as the oxidizing should be a part of the sensor model.

The switch-type  $\lambda$  sensor works like a spring. This means that the sensor voltage corresponds to the drag of the spring. When the sensor is exposed to an inert gas the springs are under a slight drag and when exposed to a lean gas composition the springs are released and the voltage drops. When the sensor is exposed to a rich gas composition the voltage is higher. These properties can be modeled with:

$$U_{\lambda st} = A_{\lambda st} + f(y_{CO}, y_{H_2}) - g(y_{O_2}). \quad (6.14)$$

$A_{\lambda st}$  corresponds to the value when no reducing nor oxidizing species are present.

An analysis in [3] has shown that the sensor output corresponds with the logarithm of the exhaust gas components. When exposed to rich exhausts the sensitivity to  $H_2$  is dominating, however even though there is no  $H_2$  present the sensor shows a higher input than when exposed to an inert gas. The sensor output also decreases with increasing temperatures. A model that covers these considerations is:

$$U_{\lambda st} = A_{\lambda st} + E_{A,\lambda st} \cdot e^{\frac{-E_{A,\lambda st}}{RT_{tp}}} \cdot \log_{10}(1 + B_{\lambda st}y_{CO} + C_{\lambda st}y_{H_2}) - F_{\lambda st} \cdot \log_{10}(1 + D_{\lambda st}y_{O_2}). \quad (6.15)$$

When the concentrations are zero the corresponding term should also become zero and thus the 1 in the logarithmic expressions. The 1 also prevent the terms from becoming negative.

The exhaust gas in the real sensor is brought to a chemical equilibrium and thus the model cannot be applied to the concentrations directly. The calculation of the equilibrium concentrations is very complex and a crude approximation is used. When the mixture is lean the concentrations are:

$$\begin{aligned} y_{O_2} &= \max(y_{O_2}^{tp} - 0.5(y_{H_2}^{tp} + y_{CO}^{tp}), 0) \\ y_{CO} &= 0 \\ y_{H_2} &= 0 \end{aligned} \quad (6.16)$$

and a somewhat more complicated calculation when the inlet is rich:

$$\begin{aligned} y_{O_2} &= 0 \\ y_{CO} &= \max(y_{CO}^{tp} - 2(1 - w_{\lambda st})y_{O_2}^{tp} + \min(y_{H_2}^{tp} - 2w_{\lambda st}y_{O_2}^{tp}, 0), 0) \\ y_{H_2} &= \max(y_{H_2}^{tp} - 2w_{\lambda st}y_{O_2}^{tp} + \min(y_{CO}^{tp} - 2(1 - w_{\lambda st})y_{O_2}^{tp}, 0), 0). \end{aligned} \quad (6.17)$$

It is assumed that CO has a higher inclination to react with the excess  $O_2$  as compared to  $H_2$  and the weighing factor  $w_{\lambda st}$  is introduced to take that into account.  $w_{\lambda st}$  was chosen as:

$$w_{\lambda st} = \frac{0.3y_{H_2}^{tp}}{0.3y_{H_2}^{tp} + y_{CO}^{tp}}. \quad (6.18)$$

The response time of the sensor is much shorter than the dynamics of the exhaust gas composition. Thus the sensor dynamics can be neglected and the presented algebraic model should be sufficient.

## 6.2 Parameter estimation

The model contains many parameters. Most of the physical parameters have been found in tables or in the data sheets of the catalytic converter. However, the parameters not found must be estimated. These

parameters are the switch-type  $\lambda$ -sensor specific parameters, the oxygen storage capacity and heat-transfer coefficient between the TWC and ambient, the kinetic parameters of the TWC and heat conductivity in the solid phase.

If measurements of the concentrations downstream of the catalytic converter are available, the  $\lambda$ -sensor parameters can be found separately which makes the estimation of the rest of the parameters much easier.

Unfortunately, concentration measurements were not available in the laboratory used for measurements in this thesis and therefore the parameters are quite hard to obtain.

### 6.2.1 Simplifications and assumption

To make the parameter estimation more accurate a few assumptions and simplifications can be made to get better start values to use with the estimation algorithm.

#### Obtaining the lean-related parameters in the $\lambda$ -sensor model

When the engine has been running lean long enough to fill the TWC with oxygen the downstream exhausts can be assumed to be the same as the inlet gases, which means that the inlet concentrations can be applied directly to the  $\lambda$ -sensor model. If assuming that  $A_{\lambda st}$  has the same value as in [3] a least-square optimization routine can be applied and  $D_{\lambda st}$  and  $F_{\lambda st}$  can be obtained.

#### $B_{\lambda st}$ and $C_{\lambda st}$ ratio

A constant ratio between  $B_{\lambda st}$  and  $C_{\lambda st}$  can be assumed. This ratio is assumed to be the same as in [3]

#### Fixed heat transfer and heat conduction

The heat transfer coefficient between the converter and the ambient air,  $\alpha_{cat}$ , can at first be set to zero. This will make the temperatures increase but the change is not dramatic. The heat conduction  $\lambda_s$  is important, though a high accuracy is not needed due to the fact that the model is very simplified. Hence a reasonable value can be used.

### 6.2.2 Estimation algorithm

Many of the parameters that has to be estimated are dependent on each other and therefore an estimation algorithm has been made in order to get as accurate parameter values as possible. The optimization algorithm needs good first guesses. The algorithm should first be applied to the kinetic parameters, SC,  $B_{\lambda st}$ ,  $E_{A,\lambda st}$  and  $E_{E\lambda st}$  with the rest

of the values as suggested in section 6.2.1. Now the parameters have been narrowed down from 22 to 16. Next step is to freeze a few of the parameters at the time and apply the algorithm to the rest. This is done in order to make the parameters which are dependent on other parameters evolve without interacting with each other. An example of the estimation algorithm is given below:

1. kinetic parameters  $A_i$  and  $E_i$ , SC,  $B_{\lambda st}$ ,  $E_{A,\lambda st}$  and  $E_{E\lambda st}$
2. kinetic parameters only
3.  $B_{\lambda st}$ ,  $E_{A,\lambda st}$  and  $E_{E\lambda st}$  only
4. SC only
5. all parameters, including  $A_{\lambda st}$ ,  $C_{\lambda st}$ ,  $D_{\lambda st}$ ,  $F_{\lambda st}$ ,  $\alpha_{cat}$ ,  $\lambda_s$
6. kinetic parameters only
7. sensor parameters only
8.  $\alpha_{cat}$
9. SC
10.  $\lambda_s$

The parameters are obtained by minimizing the error between the model output and the switch-type  $\lambda$ -sensor. Some parameters however, e.g  $\alpha_{cat}$ , affects the temperature rather than the model output, hence when  $\alpha_{cat}$  is estimated the least-square algorithm should minimize the error between the models temperature in the TWC and the sensor value instead of the switch-type  $\lambda$ -sensor.

If the result is not satisfying or if no good initial values are available the steps should of course be repeated.

The values obtained can be found in appendix C.

### 6.3 Validation

Two sets of parameters are presented in this chapter. The first set gives an output which is more alike the  $\lambda$ -sensor output than the second set, at least in the beginning of the simulations. The second set gives the states a more realistic appearance than the first. The major difference between the first and second parameter set is that a parameter representing the lambda offset had a fix value in the second set but not in the first, when estimating the parameters.

The parameters (from both sets) have initially been obtained as described above. The steps have been repeated several times.

### 6.3.1 The first set

When estimating the first set of parameters, a parameter representing the wide-range  $\lambda$ -sensor offset was included in the estimation algorithm. This parameter was finally estimated to be 0.001, but this is not a reasonable value. As implied in section 2.2 the offset should be approximately -0.01.

As mentioned above the first set of parameters gives an output that is similar to the sensor output, at least during the first 290-300 seconds. Figure 6.2 shows the measured and simulated switch-type  $\lambda$ -values after the converter from the four sets of validation data. As can be seen, the

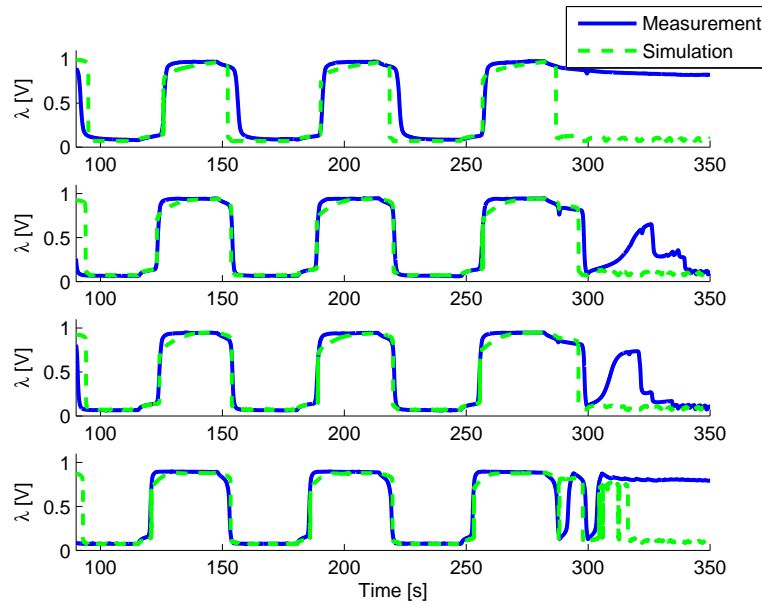


Figure 6.2: Simulated and measured switch-type  $\lambda$ -sensor values from the four sets of measurements.

model can describe the output well, except when the input  $\lambda$  changes fast (290s-350s).

Looking at the states describing the oxygen and carbon monoxide levels stored in the converter (see figure 6.3), it is can be seen that the model not describe the dynamics of the converter in a physical way. When the engine has been running lean for a long time the converter is filled with oxygen; the oxygen storage level is 1. As can be seen in figure 6.3 this is described by the converter. However, when the engine has been running rich for a long time the oxygen level should decrease to zero as the excess reducing species react with the oxygen in the

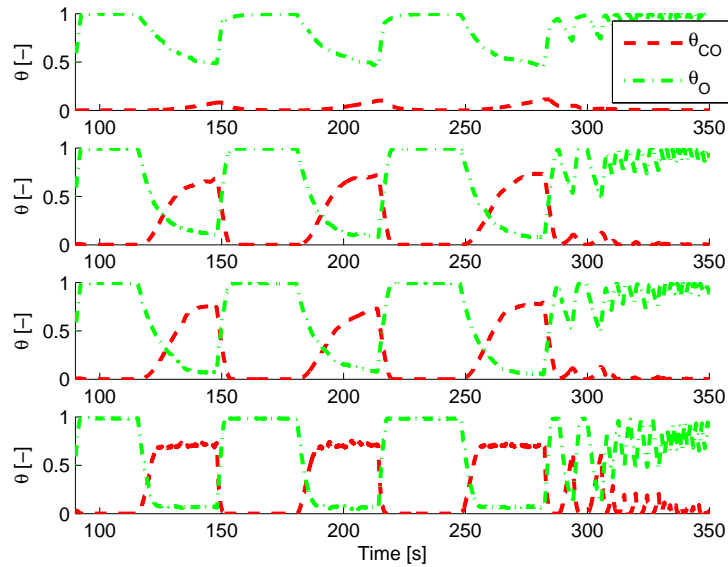


Figure 6.3: Simulated levels of O and CO in the first cell.

converter. This is not described by the model, since the oxygen level in the simulation from e.g. operating point 1 never is below 0.5. In the simulations from the other data sets the oxygen level is less than 0.5 at the lowest point, but the same parameters should be able to describe this in all operating points.

It is hard to say how much the carbon monoxide level should increase when running rich. It is though reasonable that it should increase, as the engine then produces more of the reducing species. Naturally, the carbon monoxide level should also decrease when the engine starts to run lean again. Hence, looking at figure 6.3, the carbon monoxide level described by the model is reasonable. The levels of oxygen and carbon monoxide in the other cells behave as the ones in the first cell.

### 6.3.2 The second set

The second set of parameters were estimated with a fixed value of the wide-range  $\lambda$ -sensor offset, -0.01. This resulted in model states that are more physically representative than with the first set of parameters. Figure 6.4 shows the simulated levels of oxygen and carbon monoxide in the first cell. As can be seen in the figure, the simulated oxygen levels are changing as desired, i.e. they go up to 1 when the engine has been running lean for a while and they all drop down to zero after

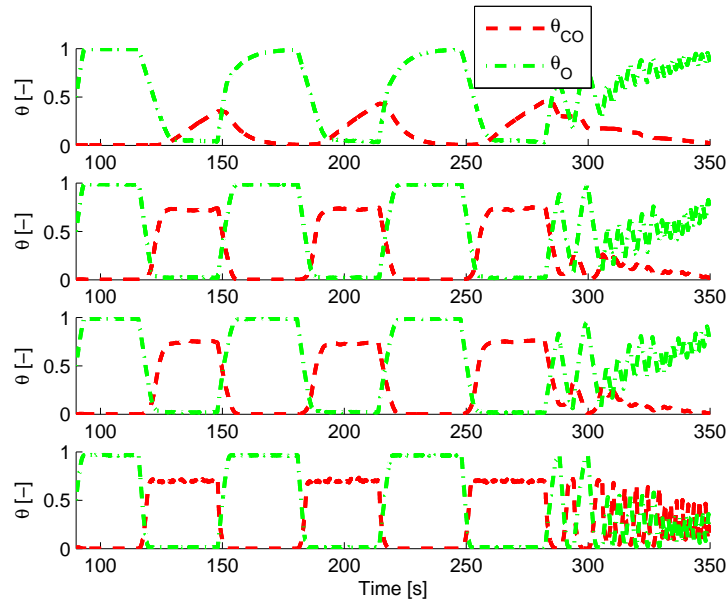


Figure 6.4: Simulated levels of O and CO in the first cell.

running rich for a while. The carbon monoxide levels also acts as expected. However, even though the states behave as expected, the output switch-type  $\lambda$ -value does not match with the measured value as well as in [3]. Figure 6.5 shows the simulated and measured switch-type  $\lambda$ -value. It can be seen that these parameters do not describe the time when  $\lambda$  switches from lean to rich or from rich to lean as good as the first set of parameters. The second set though, is better at describing the output when the input  $\lambda$  switches fast.

### 6.3.3 Number of cells

Since the estimation of the parameters have been very time-demanding, tests on how the accuracy changes with the number of cells used in the TWC model have not been made, as changing the number of cells also means that new parameter values have to be obtained. As Auckenthaler [3] has found that three cells are suitable in terms of both accuracy and CPU power, the same number of cells have been chosen in this thesis as well.

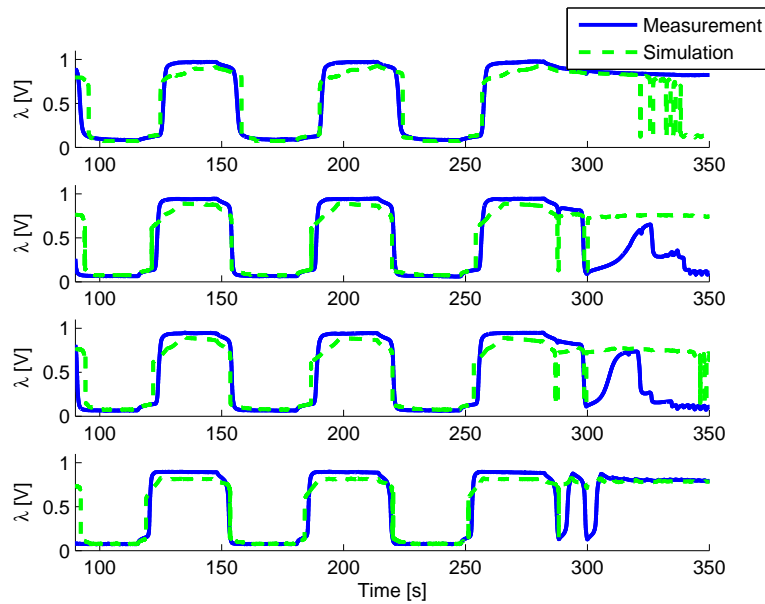


Figure 6.5: Simulated and measured switch-type  $\lambda$ -sensor values from the four sets of measurements.

### 6.3.4 Discussion

One important aspect when modeling, is to think about what the model is going to be used for. In this case, it is desired to use the model for estimating the oxygen storage for control purposes, i.e. it will be used together with a Kalman filter to observe the oxygen storage. This means that it is very important that the oxygen storage level and carbon monoxide level states are good reflections of the real levels. However, it is also crucial that the switch-type  $\lambda$ -value agrees well with the measured, since the states are being corrected based on the difference between the simulated and measured value. Based on this, the first parameter set is not suitable to use in a Kalman filter. Since the second set of parameters shows better agreement between measured and simulated values and also describes the states better, the second set should be chosen if the model is to be used in a Kalman filter.

# Chapter 7

## Model comparison

One reason to compare the models is to decide whether any of the models can be used in the online adaption strategy described in the following chapter.

### 7.1 Accuracy of the models

An important aspect when comparing the models is their accuracy compared to measurements.

#### Model A

It is hard to draw any conclusions about the accuracy of the catalytic converter model in chapter 4, since a reliable wide-range  $\lambda$ -sensor downstream of the converter, or a  $\lambda$  converter model with high accuracy is needed to compare the model with measured data.

With the  $\lambda$  converter used in this thesis, the model of the converter seems to capture the dynamics of the converter well for one operating point, but the model is not expected to show as good results when the operating point is changed or the converter is aged.

#### Model B

Since no simulations has been done with this model there is no information available about the accuracy of the model.

#### Model C

The accuracy of the Model C output as compared to measurements is good, regarding the low complexity of the model. It describes the long-period changes in inlet  $\lambda$  well, but the agreement when the inlet  $\lambda$

changes fast is not very good. The oxygen level and carbon monoxide states changes in a reasonable way.

### Comparison

The accuracy of Model A and Model C is almost the same, as can be seen in figures 4.3 and 6.5. The accuracy of Model C is though expected to be better than Model A in other operating points than used for evaluation in this thesis, since the model is based on physical reactions in the converter.

## 7.2 Inputs and outputs

Due to economical reasons, automotive producers is reluctant to add additional sensors. Therefore a model using only the present sensors is desirable.

### Model A

The catalytic converter model described in chapter 4, uses measurements from a wide-range  $\lambda$ -sensor before the catalytic converter, and the fuel mass flow as inputs. The output, which is to be compared with measurements, from the model of the catalytic converter is a wide-range  $\lambda$ -value. When the  $\lambda$ -converter model is applied however, a switch-type  $\lambda$ -value is the output. The  $\lambda$ -converter model also needs exhaust gas temperature as input.

### Model B

Model B takes the upstream wide-range  $\lambda$  as input and the output is the downstream wide-range  $\lambda$ .

### Model C

Model C takes the wide-range  $\lambda$ , exhaust mass flow and exhaust temperature as inputs. The output is a switch-type  $\lambda$ -value.

### Comparison

The major difference in the models' need for extra sensors, is the use of a wide-range or a switch-type  $\lambda$ -sensor downstream of the converter. The measurements of the mass flow and exhaust gas temperatures are of minor concerns. Hence, from this point of view, Model A and C are preferred.

## 7.3 Number of states and parameters

The number of parameters is important because a higher number indicates that a good estimation of the parameters is harder to obtain. This in turn makes it hard to apply and adjust the model to different catalytic converters.

The number of states is a measurement of how detailed the model is. Additionally the CPU recourses demanded by an online adaption strategy, such as the one described in chapter 8, is linked to the number of states together with the number of parameters that changes as a result of the ageing of the converter.

### Model A

Model A contains two states describing the oxygen storage and the reversible catalyst deactivation. These correspond to the states in Model C describing the occupancy of O and CO. A big difference is that no consideration has been made to describe the spatially distributed nature of the converter in this model.

The model of the catalytic converter contains nine parameters. Additionally the  $\lambda$  converter introduce ten parameters that have to be estimated. Among the nine parameters in the model of the converter there are six which change as the catalytic converter ages.

### Model B

Model B has only one state, which indicates the current global relative oxygen coverage of ceria (ROC) in the catalytic converter. ROC corresponds to the storage capacity SC in Model C. Model B has two functions that easily can be estimated with a data set where the ROC goes from 0 to 1 and from 1 to 0. Furthermore, the model has one additional parameter that has to be estimated. This parameter is easy to obtain using the same data sets as for the functions. Both parameter and functions change over time and can be estimated online. Good sensor values must be available in order to estimate the parameter and functions.

### Model C

The dynamics of the converter is in Model C described by the TWC model. Each cell in the TWC model contains three states, describing the occupancy of O and CO, and the solid phase temperature. In this case when the catalytic converter is divided into three cells there are consequently nine states.

The exhaust gas model, the TWC model and the sensor model have together 22 parameters which need to be estimated. Amongst them there is one which changes as the catalytic converter ages.

### Comparison

The number of parameters that need to be estimated are 19 in Model A, 1 in Model B, and 22 in Model C. Model B additionally contains 2 functions with parameters, but these are obtained by simple calculations, and does not demand any optimization. Estimating the parameters in Model A and Model C, is hence expected to cause more trouble, than the estimation for Model B.

In an online strategy two states and 6 parameters would have to be estimated if Model A was to be used. One state, the parameter and two functions would have to be estimated if using Model B. The same numbers for Model C is 9 states and one parameter. From this, the conclusion that Model B is least demanding if it were to be implemented in an online strategy, is drawn.

## 7.4 Simulation speed

The time it takes to simulate the models is a measurement of their complexity. The shorter time it takes, the easier the model will be to fit into an engine control system. Tests have shown that a 240 s long measurement sequence takes approximately 9 seconds to simulate with Model C and approximately 4 seconds with Model A. This is not a surprising result since Model A has fewer states than Model C and hence should not need as much computer calculations as Model C.

## 7.5 Extensibility

The requirements of the models might differ depending on the field of application. It is therefore desirable to know in what extent the models can be modified or extended.

### Model A

Model A is empirical, and the dynamics of the TWC is assumed to be dominated of the oxygen storage and the reversible catalyst deactivation. Extending this model with further characteristics would probably result in the need to reconsider the entire model.

### Model B

The model can easily be extended to be accurate in a wider operating range by making the parameter and functions depend on the exhaust mass flow. However, that also means that the model needs one more input.

### Model C

Since Model C is a simplified physical model, it is quite easy to extend. One way is to include humid air or a gasoline containing not only H and C, but also O in the combustion reactions (6.1) and (6.2).

It is also likely that the model can be extended with the NO and HC concentrations without a drastic increase of the CPU power.

### Comparison

Model C originates from a more advanced model, which has been simplified in order to be used in control strategies or on board diagnostics. More about the advanced model can be read in [3]. It is hence quite easy to extend. Even though Model B is a black-box model, it can be extended to show better results with different mass flows.

## 7.6 Final comparison

The most important aspect when comparing the models, is of course the accuracy compared to measurements. If the model makes a poor description of the catalytic converter, it does not matter if e.g. the demand for CPU power is limited.

Model B has due to offset problems with the sensors not been implemented and thus it cannot be used in the online adaptation strategy.

Model C is expected to be more accurate than Model A in other operating point than the ones used in this thesis.

Model C contains the highest amount of states, and is hence the most CPU consuming model. Additionally it is the model where the parameter values are hardest to obtain. On the other hand, the many states and parameters make the model more reliable when it comes to describing the behavior of the catalytic converter, and Model C has the most physical interpretation of the three models.



## Chapter 8

# Extended Kalman filter

To be able to use the models of the catalytic converter from the previous chapters, both the estimation of the internal state variables, by means of an observer, and the estimation of the parameters that changes over the converter's lifetime, should be performed by the control unit during operation, i.e. an online adaption strategy is required.

The correct estimation of the controlled internal state variables such as the oxygen storage level require a fast and accurate adaption to the "true" values. One way to achieve this is to use an extended Kalman filter (EKF), which can handle both the internal state variables and adapting parameters, as well as the nonlinear models.

### 8.1 Introduction to EKF

The EKF in this chapter is implemented accordingly to the EKF presented in [3]. Therefore, only a short introduction is given. For further information on the subject the reader is referred to [3], and books and papers on the subject such as [5] and [13].

Assume that the process noise and the measurement noise processes are uncorrelated, zero-mean white noise and additive to the state derivative and the output vectors. Then the system can be described by nonlinear state space equations:

$$\begin{aligned}\dot{\mathbf{x}} &= \mathbf{f}(\mathbf{x}, \mathbf{u}) + \mathbf{w} \\ \mathbf{y} &= \mathbf{h}(\mathbf{x}, \mathbf{u}) + \mathbf{v},\end{aligned}$$

where  $\mathbf{u}$  is the control input vector,  $\mathbf{x}$  the state vector,  $\mathbf{y}$  the output vector,  $\mathbf{w}$  the process noise and  $\mathbf{v}$  the measurement noise. The covariance matrices for the process and the measurement noise can be

expressed as:

$$\begin{aligned}\mathbf{Q} &= E[\mathbf{w}\mathbf{w}^T] \\ \mathbf{R} &= E[\mathbf{v}\mathbf{v}^T],\end{aligned}$$

and the covariance matrix of the estimate error as:

$$\mathbf{P} = E[(\mathbf{x} - \hat{\mathbf{x}})(\mathbf{x} - \hat{\mathbf{x}})^T].$$

The model has to be linearized around the current state estimate  $\hat{\mathbf{x}}$  to obtain the systems measurement matrix  $\mathbf{H}$ :

$$\mathbf{H} = \left. \frac{\partial \mathbf{h}(\mathbf{x}, \mathbf{u})}{\partial \mathbf{x}} \right|_{\mathbf{x}=\hat{\mathbf{x}}}$$

and the dynamics matrix  $\mathbf{F}$ :

$$\mathbf{F} = \left. \frac{\partial \mathbf{f}(\mathbf{x}, \mathbf{u})}{\partial \mathbf{x}} \right|_{\mathbf{x}=\hat{\mathbf{x}}}.$$

Since the purpose is to create a discrete filter, the fundamental matrix  $\Phi_k$  is required instead of the systems dynamic matrix.  $\Phi_k$  can be approximated by the first two terms of the Taylor-series expansion:

$$\Phi_k = e^{\mathbf{F}h_s} \approx \mathbf{I} + \mathbf{F}h_s$$

The first step of the extended Kalman filter algorithm is the "time update" or "extrapolation" step, where the state vector estimate  $\hat{\mathbf{x}}$  and the covariance matrix  $\mathbf{P}$  are projected one step ahead:

$$\hat{\mathbf{x}}_k^- = \mathbf{f}(\hat{\mathbf{x}}_{k-1}, \mathbf{u}_{k-1}) \quad (8.1a)$$

$$\mathbf{P}_k^- = \Phi_k \mathbf{P}_{k-1} \Phi_k^T + \mathbf{Q}_k, \quad (8.1b)$$

where the discrete process noise matrix  $\mathbf{Q}_k$  can be obtained from the continuous matrix  $\mathbf{Q}$  by integration over one time step:

$$\mathbf{Q}_k = \int_{(k-1)h_s}^{kh_s} \Phi(\tau) \mathbf{Q} \Phi^T(\tau) d\tau$$

The second step is the "measurement update" or "correction" step, where the state vector estimate  $\hat{\mathbf{x}}$  and the covariance matrix  $\mathbf{P}$  are corrected using the error between the projected output vector  $\mathbf{h}(\hat{\mathbf{x}}_k^-)$  and the measured vector  $\mathbf{z}_k$ , and the measurement matrix  $\mathbf{H}_k$ :

$$\hat{\mathbf{x}}_k = \hat{\mathbf{x}}_k^- + \mathbf{K}_k(\mathbf{z}_k - \mathbf{h}(\hat{\mathbf{x}}_k^-, \mathbf{u}_k)) \quad (8.2a)$$

$$\mathbf{P}_k = (\mathbf{I} - \mathbf{K}_k \mathbf{H}_k) \mathbf{P}_k^- \quad (8.2b)$$

The Kalman gain  $\mathbf{K}_k$  is calculated from the discrete Riccati-equation:

$$\mathbf{K}_k = \mathbf{P}_k^{-1} \mathbf{H}_k^T (\mathbf{H}_k \mathbf{P}_k^{-1} \mathbf{H}_k^T + \mathbf{R}_k)^{-1} \quad (8.3)$$

The filter algorithm is established with equations (8.1)-(8.3). These equations need to be calculated every time step. Hence, the amount of CPU power that is needed to carry them out has to be **rather small**. With this in mind, one might think that what appears to be a matrix inversion in the Riccati equation (8.3) could cause problems, but a closer inspection reveals that this is actually a scalar inversion, in this case, since the output vector is one dimensional. (**Bara en utsignal**)

### 8.1.1 Parameter identification

The parameters that change over the catalytic converter's lifetime need to be identified online. This is easily implemented when a discrete EKF is used by seeing them as additional state variables.

The discrete state space equation is originally expressed as:

$$\begin{aligned} \mathbf{x}_{k+1} &= \mathbf{f}(\mathbf{x}_k, \mathbf{u}_k) + \mathbf{w}_k \\ \mathbf{y}_k &= \mathbf{h}(\mathbf{x}_k, \mathbf{u}_k) + \mathbf{v}_k, \end{aligned}$$

and then augmented with the equation for the new state variables

$$\mathbf{p}_{k+1} = \mathbf{p}_k + \mathbf{w}_{p,k},$$

where  $\mathbf{p}$  denotes the vector with the new state variables and  $\mathbf{w}_{p,k}$  is a zero-mean scalar white noise process. The effect of this is that  $\mathbf{p}$  is kept constant in the extrapolation step and only adjusted in the measurement update step. Obviously  $\mathbf{Q}$  and  $\mathbf{P}$  have to be augmented accordingly.

## 8.2 Implementation

In this thesis, as well as in [3], the model incorporated in the EKF is the Model C.

As a discrete EKF is used, the model has to be discretized. One way to do this is to approximate the expressions for the states in the catalytic converter model with an Euler forward scheme.

When using Model C, the input, state and output vectors are de-

defined as follows:

$$\mathbf{u} = \begin{bmatrix} \lambda \\ \dot{m}_{exh} \\ T_{exh} \end{bmatrix}, \quad \mathbf{x} = \begin{bmatrix} \theta_{O,1} \\ \theta_{CO,1} \\ T_{s,1} \\ \theta_{O,2} \\ \theta_{CO,2} \\ T_{s,2} \\ \theta_{O,3} \\ \theta_{CO,3} \\ T_{s,3} \end{bmatrix}, \quad \mathbf{y} = [U_{\lambda st}]$$

The discrete form of the state space model is augmented with the parameter that needs to be identified,  $SC$ , which is the parameter that changes as the converter ages:

$$SC_{k+1} = SC_k + w_{SC,k}$$

Hence the model now contains ten state variables. This is close to the allowed upper limit. As stated before it should be simple enough to fit in the control system.

Since the coupling between the temperatures and the sensor output is relatively weak the filter can be simplified by not including the temperatures in the measurement update step. The temperatures are hence only calculated in the extrapolation step and then handled as model parameters.

The state vector can thus be split in two vectors

$$\mathbf{x}_{corr} = \begin{bmatrix} \theta_{O,1} \\ \theta_{CO,1} \\ \theta_{O,2} \\ \theta_{CO,2} \\ \theta_{O,3} \\ \theta_{CO,3} \\ SC \end{bmatrix} \quad \text{and} \quad \mathbf{x}_{Temp} = \begin{bmatrix} T_{s,1} \\ T_{s,2} \\ T_{s,3} \end{bmatrix}.$$

These two vectors in combination is used with an Euler forward scheme to calculate the state vector in the extrapolation step, but only  $\mathbf{x}_{corr}$  is updated in the correction step.

An attempt to calculate the Jacobians  $\mathbf{F}$  and  $\mathbf{H}$  analytically was made, but this task turned out to be too awkward, and they are here calculated numerically with a forward differential scheme.

### 8.3 Tuning of the EKF

The two covariance matrices  $\mathbf{Q}$  and  $\mathbf{R}$  are used as tuning parameters of the EKF. If  $\mathbf{R}$  is chosen large as compared to  $\mathbf{Q}$ , the measured value is

supposed to be less accurate than the estimated value from the model, and hence the model is trusted more. Correspondingly, the opposite is true, if  $\mathbf{Q}$  is chosen to be large and  $\mathbf{R}$  small.

According to [3], the model noise should generally be considered as small compared to the measurement noise, because a relatively slow adaptation is preferred.

## 8.4 Discussion and results

Due to lack of time, the implementation of the EKF has not been fully investigated. This description of how to implement the EKF should be looked upon as a suggestion of how to start if an online adaptation strategy is to be used.

### 8.4.1 Validation

The results from a simulation with the EKF can be seen in figure 8.1 and 8.2. As can be seen, the switch-type  $\lambda$ -value follows the measured one well, the  $\theta_O$  seems to have the expected behavior, but  $\theta_{CO}$  acts in an unexpected way in this simulation. It should be emphasized that this is a simulation, with particularly good results. A small change in any value such as  $\mathbf{Q}$ ,  $\mathbf{R}$  or the initial value of a state results in considerably deteriorations.

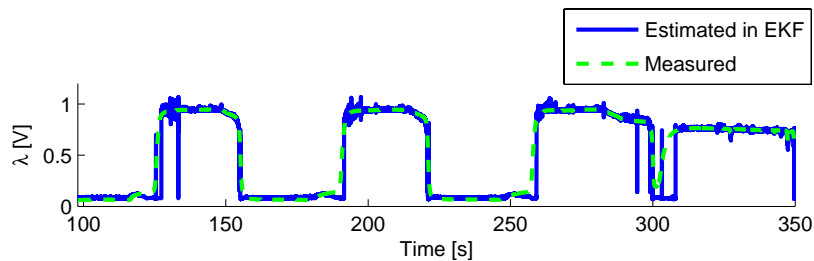


Figure 8.1: The measured switch-type  $\lambda$  and the switch-type  $\lambda$ -value estimated by the model in the EKF.

These problems might be numerical, because the simplest method always was chosen e.g. when the model was discretized, and when the Jacobians  $\mathbf{F}$  and  $\mathbf{H}$  were estimated. This did not lead to any major numerical problems in [3]. In this thesis however, the EKF has been run with a sample rate of 500Hz. This is higher than in a present production-type control unit, but only half of the sample rate used in [3]. Additionally, the parameter values in [3] is expected to have greater accuracy than the ones obtained in this thesis.

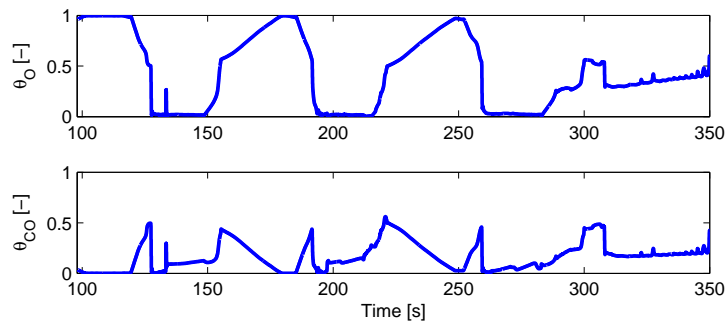


Figure 8.2: The upper plot shows  $\theta_O$ , and the lower  $\theta_{CO}$ , in the EKF.

The comparatively good result should hence not be seen as something that is always achieved, but rather as a confirmation that good results are possible to obtain.

### 8.4.2 Properties of the EKF

Provided that the previously described problems have been handled, is the introduced EKF reliable in all situations? Is for example the system stable and observable, and simple enough to fit in the control system? These properties have been investigated in [3], and will only be mentioned shortly here.

#### Splitting the state vector

As described in the previous section the state vector is split and hence the temperatures are not included in the measurement update step. This is done to simplify the filter, but does it also reduce the accuracy? Actually, it was shown in [3] that this reduction of the problem considerably improves the robustness of the filter against sudden transients, because of the weak coupling between the temperatures and the sensor output.

#### Stability

The system is obviously bounded-input/bounded-output stable, and all state variables are bounded. This can be seen since the system focused on here describes a physical system with physically limited occupancies, which can not become negative and their sum can not exceed 1. The temperature can never decrease below the ambient temperature and the heat production is dependent on the occupancies and therefore cannot increase indefinitely. Thus, all state variables remain bounded in the

real system and since the model is a representation of the reality, they remain bounded in the model as well. According to [3], the resulting linearized system is asymptotically stable in any steady state operating point.

When the model is implemented in an EKF however, it is possible that the states is adjusted to values outside their physical limitations. One way to try to come around this is to implement boundaries in the EKF, which also has been done. This might be another reason to the strange behavior of  $\theta_{CO}$ , since it primarily occurs when there is supposed to be higher levels of  $\theta_{CO}$ .

### Observability

To investigate the observability, a comparison between the model consisting of three connected cells and two occupancies, and a system of three tanks filled with e.g. water and oil, is made in [3]. If each tank leaks water/oil to the next tank dependent on the level of the liquid, and the size and geometry of the tanks are known, as well as the correlation of the storage levels and the leakage, it is intuitively obvious that the levels of water and oil in the three tanks can be determined if the amount of water and oil leaving the last tank is measured.

### Convergence

The investigation of the convergence is done in a similar way as with the observability in [3]. A system consisting of a tank with entering and leaving mass flows is used to conclude that the system has to be excited to guarantee convergence of the Kalman filter states to the "true" values. Under steady state conditions, when the input and output mass flows are equal and constant, it is clear that the volume of the tank cannot be determined. In the model it is theoretically possible to determine the storage capacity under steady state conditions, since the reaction rates and hence both the heat production and the tailpipe concentrations are dependent on SC. But this input-output link is weak.

The condition for convergence is hence that the system has to be excited. This is however usually not a problem. The disturbances of the  $\lambda$  at the TWC inlet and the transients of the exhaust gas mass flow during normal driving conditions are sufficient. The worst case scenario is when the driving is constant during longer periods, e.g. when driving on a highway. In that case the excitations can become very weak, but at least the process does not diverge.



## Chapter 9

# Results and Discussion

The purpose of this thesis was to examine the possibilities to model the dynamics of a catalytic converter for control purposes. During the search for existing models, three promising models were found and they have been investigated in this thesis.

All three models have the wide-range  $\lambda$  as input and have at least one state that in some way describes the oxygen storage level, and they all consider catalyst deactivation. The three models are fairly simple and needs online adaptation due to ageing of the converter. A short summary of the most important features of the models are presented below. Further comparison of the models is given in chapter 7.

Two of the models (Model A and Model B) have a wide-range  $\lambda$  as output. To be able to compare the values from these models with measurements, the wide-range  $\lambda$ -sensor downstream of the catalytic converter have to be accurate enough. This is a problem since wide-range sensors often suffers from time varying biases. More about the disadvantage of a wide-range sensor downstream of the converter can be found in section 3.3. The third model (Model C), on the other hand, has a switch-type  $\lambda$  as output.

Of the three models, Model B would probably be the one that demands the least CPU power and it is the easiest one to adapt to different kinds of converters. No expensive tests or optimization routines have to be done to obtain the parameter and functions. However, it is also the most sensitive model by means of the characteristics of the  $\lambda$ -sensors. The dynamics in Model B is based on the wide-range sensor values before and after the converter, and when the sensors do not behave as expected the model works poorly. The sensor problem is hard to get around, since an accurate converter model from switch-type to wide-range  $\lambda$ -value is difficult to make, because of the nonlinearity of the switch-type sensor.

Model A describes the oxygen level well, but the  $\lambda$ -sensor value

after the converter is not reliable, which is crucial if the model is to be used for control purposes. To overcome this, the original TWC model has been extended with a model that converts the output wide-range  $\lambda$  into a switch-type  $\lambda$ . This gives a better result, but it is not expected to extrapolate to other operating points than the ones used for the parameter estimation.

Model C is the most detailed of the three models examined, it is thus no surprise that it is the most accurate, consume the highest amount of CPU power, and contains the highest number of parameters. Even though the results in this investigation is not as good as the results in [3], it is the most promising of the three models presented in this thesis. The drawback of Model C is that it has many parameters that are hard to estimate if only the switch-type  $\lambda$ -sensor is available for measurements. If sensors measuring the concentrations of the species after the converter are available, the parameter estimation can be divided into two parts, and thus the identification of the parameters is easier.

The extended Kalman filter presented in chapter 8, together with Model C, is not fully investigated and should be considered as a way to start if an online adaption strategy is to be implemented. The use of an EKF is promising, and good results are expected if the previously described numerical problems (see section 8.4.1) are seen to.

An important conclusion drawn from this thesis, is that the behavior of the sensors have to be taken into account if a model of the converter is to be used e.g. for onboard control.

Finally, the chances are good that the extended Kalman filter together with Model C can successfully be used in an engine control system, if an effort is made to tune in the model parameters even better and the problems with the EKF is solved.

## Chapter 10

# Future work

First of all, more time should be invested in obtaining parameter values for Model C that describe the dynamics more accurately, e.g by using other estimation algorithms or investigate if any simplifications like the ones in section 6.2.1 can be done. When satisfying results have been obtained, the next step is to solve the problems in the extended Kalman filter and finally, test the filter online with a control strategy. Since the storage capacity is adapted online the filter can be used for diagnostic purposes as well.

As described in previous chapters, the reactions taking place in the converter make the gas composition change dynamically. As the gas composition has great impact on the sensors' behavior, further investigation of the  $\lambda$ -sensors are highly recommended, especially if a wide-range  $\lambda$ -sensor is to be used. Additionally, the effects of sensor ageing should be examined.



# References

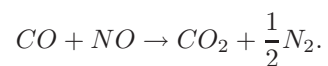
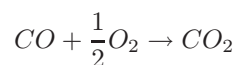
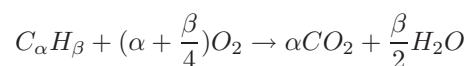
- [1] Division of vehicular systems, lab. Internet site. <http://www.fs.isy.liu.se/Lab/>, visited June 2005.
- [2] Laborationskompendium gröna bilen - reglerteknik för fordon. Lab compendium, Division of Vehicular Systems, Department of Electrical Engineering, Linköpings Universitet, Linköping, Sweden, 2004. In Swedish.
- [3] T. Auckenthaler. *Modelling and Control of Three-Way Catalytic Converters*. Phd thesis, June 2005.
- [4] Mario Balenovic. *Modeling and Model-Based Control of a Three-Way Catalytic Converter*. Phd thesis, Technische Univeriteit Eindhoven, 2002.
- [5] Lennart Ljung Fredrik Gustafsson and Mille Millnert. *Signalbehandling*. Studentlitteratur, Lund, Sweden, 2 edition, 2001. In Swedish.
- [6] James C. Peyton Jones. Modeling combined catalyst oxygen storage and reversible deactivation dynamics for improved emissions prediction. SAE paper 2003-01-0999, 2003.
- [7] James C. Peyton Jones. A novel approach to catalyst obd. SAE paper 2005-01-0024, 2005.
- [8] Kenneth R. Muske and James C. Peyton Jones. Feedforward/feedback air fuel ratio control for an automotive catalyst. In *Proceedings of the American Control Conference*, volume 2, pages 1386–1391, Denver, Colorado, June 2003.
- [9] Kenneth R. Muske and James C. Peyton Jones. Estimating the oxygen storage level of a three-way automotive catalyst. In *Proceedings of the American Control Conference*, volume 5, pages 4060 – 4065, Boston, Massachusetts, June 2004.

- 
- [10] Lars Nielsen and Lars Eriksson. *Course material Vehicular Systems*. Linköping, Sweden, 2004.
  - [11] Christopher H. Onder Theophil S. Auckenthaler and Hans P. Geering. Aspects of dynamic three-way catalyst behaviour including oxygen storage. In *Proceedings of the IFAC Symposium on Advances in Automotive Control*, University of Salerno, Italy, April 2004.
  - [12] Christopher H. Onder Theophil S. Auckenthaler and Hans P. Geering. Online estimation of the oxygen storage level of a three-way catalyst. SAE paper 2004-01-0525, 2004.
  - [13] Greg Welch and Gary Bishop. An introduction to the kalman filter. Technical Report TR 95-041, Department of Computer Science, University of North Carolina, Chapel Hill, US, April 2004. [http://www.cs.unc.edu/~welch/media/pdf/kalman\\_intro.pdf](http://www.cs.unc.edu/~welch/media/pdf/kalman_intro.pdf), visited June 2005.

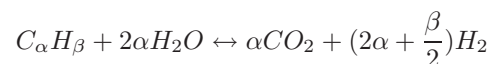
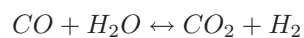
## Appendix A

# Chemical reactions

The main purpose of a catalytic converter is to promote the following three chemical reactions:



Additionally the TWC do not only promote these reactions, but also affects the water-gas shift and the steam-reforming reactions:



## Appendix B

# Model A - Parameter Values

The parameters of the catalytic converter in Model A are presented in table B.1. As described in chapter 4, the exhaust gas and the sensor model from chapter 6 have been merged to function as a switch-type  $\lambda$ -sensor model. The values of the parameters in this model are presented in table B.2.

Table B.1: Parameters of the catalytic converter in Model A.

<i>Parameter</i>	<i>Value</i>
$K_\lambda$	5080
$K_d$	0.314
$K_r$	0.0710
$K_\psi$	0.889
$a_1$	-1.02e-7
$a_2$	-4.78e-3
$a_3$	0.0255
$a_4$	0.105
$a_5$	0.101

Table B.2: Parameters of the switch-type  $\lambda$ -sensor in Model A.

<i>Parameter</i>	<i>Value</i>
$a_{\eta_{comb}}$	-3.06e-4
$b_{\eta_{comb}}$	4.55e-7
$\phi_{H_2/CO}$	6.48
$A_{\lambda st}$	0.238
$B_{\lambda st}$	154000
$C_{\lambda st}$	3.86
$D_{\lambda st}$	28.5
$E_{A,\lambda st}$	0.0276
$E_{E,\lambda st}$	-6990
$F_{\lambda st}$	0.0328

# Appendix C

## Model C - Parameter Values

The parameters are obtained using the algorithm described in section 6.2. The parameters in the exhaust gas model and switch-type  $\lambda$ -sensor model are presented in table C.1 and C.4, respectively. The kinetic parameters from the TWC-model are listed in table C.2 and the rest of the TWC-model parameters are listed in C.3.

When estimating the first set of parameters a parameter representing the wide-range  $\lambda$ -sensor offset was included in the estimation algorithm. This parameter was finally estimated to be 1e-3. When estimating the second set of parameters the lambda offset was assumed to be -0.01.

Table C.1: Exhaust gas model parameters

<i>Parameter</i>	<i>Value</i>	<i>Unit</i>
$a_{\eta_{comb}}$	1.765e-2	[-]
$b_{\eta_{comb}}$	-1.26e-5	[1/K]
$\phi_{H_2/CO}$	0.25	[-]

Table C.2: Kinetic parameters of the TWC model

<i>Parameter</i>	<i>1st set</i>	<i>2nd set</i>	<i>Specification/Unit</i>
E <sub>1</sub>	-20000	-18310	Activation energy [J/mol]
E <sub>2</sub>	-80	-77.56	Activation energy [J/mol]
E <sub>3</sub>	2.2e5	2.214e5	Activation energy [J/mol]
E <sub>4</sub>	2e5	2.23e5	Activation energy [J/mol]
E <sub>5</sub>	1.3e5	1.395e5	Activation energy [J/mol]
E <sub>6</sub>	1.6e5	1.597e5	Activation energy [J/mol]
A <sub>1</sub>	5	5.111	Pre-exponential factor (Langmuir-Hinshelwood) [s <sup>-1</sup> ]
A <sub>2</sub>	18	17.84	Pre-exponential factor (Langmuir-Hinshelwood) [s <sup>-1</sup> ]
A <sub>3</sub>	5.5e16	5.517e16	Pre-exponential factor (Langmuir-Hinshelwood) [s <sup>-1</sup> ]
A <sub>4</sub>	7e14	6.094e14	Pre-exponential factor (Langmuir-Hinshelwood) [s <sup>-1</sup> ]
A <sub>5</sub>	4e7	4.23e7	Pre-exponential factor (Langmuir-Hinshelwood) [s <sup>-1</sup> ]
A <sub>6</sub>	7.5e9	7.441e9	Pre-exponential factor (Langmuir-Hinshelwood) [s <sup>-1</sup> ]
$\eta_{CO}$	12		Number of sites occupied by CO

Table C.3: Geometry, material and thermodynamic parameters of the TWC model

<i>Parameter</i>	<i>Value</i>	<i>Specification/Unit</i>
$A_{geo}$	2616	Specific geometric catalyst surface [m <sup>2</sup> /m <sup>3</sup> ]
$D_{chan}$	1.117e-3	Diameter gas channel [m]
$n_c$	3	Number of discrete cells
$L_{TWC}$	152.4e-3	TWC length [m]
$dz$	$L_{TWC}/n_c$	[m]
$D_{TWC}$	118.4e-3	Catalytic converter diameter [m]
$V_{TWC}$	1.678e-3	Catalytic converter volume [m <sup>3</sup> ]
$\alpha$	82.3	Heat-transfer coefficient TWC→exhaust [W/m <sup>2</sup> *K]
$\rho_s$	1739	Density solid phase [kg/m <sup>3</sup> ]
$c_s$	906	Specific heat capacity (solid phase) [J/kg*K]
$c_p$	1100	Specific heat capacity (gas phase) [J/kg*K]
$\varepsilon$	0.73	Volume fraction of gas phase
$\lambda_s$	50	Heat conductivity solid phase [W/m*K]
$\Delta H_{H_2O}$	-241.8e3	Reaction enthalpy of H2 oxidation [J/mol]
$\Delta H_{CO_2}$	-283.0e3	Reaction enthalpy of CO oxidation [J/mol]
$\Sigma_{O_2}$	16.3	Diffusion volume
$\Sigma_{CO}$	18.0	Diffusion volume
$\Sigma_{H_2}$	6.12	Diffusion volume
$\Sigma_{N_2}$	18.5	Diffusion volume
$\alpha_{cat}$	47	Heat-transfer coefficient TWC → ambient [W/m <sup>2</sup> K]

Table C.4: Switch-type  $\lambda$ -sensor model parameters

<i>Parameter</i>	<i>1st set</i>	<i>2nd set</i>	<i>Unit</i>
$A_{\lambda st}$	0.15	0.15	[V]
$B_{\lambda st}$	4e9	3.954e9	[-]
$C_{\lambda st}$	8.8e11	8.71e1	[-]
$D_{\lambda st}$	1.028e5	102800	[-]
$E_{A,\lambda st}$	0.04455	0.04836	[V]
$E_{E,\lambda st}$	-3999	-3020	[J/mol]
$F_{\lambda st}$	0.02697	0.02697	[V]



## Copyright

### Svenska

Detta dokument hålls tillgängligt på Internet - eller dess framtida ersättare - under en längre tid från publiceringsdatum under förutsättning att inga extra-ordinära omständigheter uppstår.

Tillgång till dokumentet innebär tillstånd för var och en att läsa, ladda ner, skriva ut enstaka kopior för enskilt bruk och att använda det oförändrat för ickekommersiell forskning och för undervisning. Överföring av upphovsrätten vid en senare tidpunkt kan inte upphäva detta tillstånd. All annan användning av dokumentet kräver upphovsmannens medgivande. För att garantera äktheten, säkerheten och tillgängligheten finns det lösningar av teknisk och administrativ art.

Upphovsmannens ideella rätt innefattar rätt att bli nämnd som upphovsman i den omfattning som god sed kräver vid användning av dokumentet på ovan beskrivna sätt samt skydd mot att dokumentet ändras eller presenteras i sådan form eller i sådant sammanhang som är kränkande för upphovsmannens litterära eller konstnärliga anseende eller egenart.

För ytterligare information om Linköping University Electronic Press se förlagets hemsida: <http://www.ep.liu.se/>

### English

The publishers will keep this document online on the Internet - or its possible replacement - for a considerable time from the date of publication barring exceptional circumstances.

The online availability of the document implies a permanent permission for anyone to read, to download, to print out single copies for your own use and to use it unchanged for any non-commercial research and educational purpose. Subsequent transfers of copyright cannot revoke this permission. All other uses of the document are conditional on the consent of the copyright owner. The publisher has taken technical and administrative measures to assure authenticity, security and accessibility.

According to intellectual property law the author has the right to be mentioned when his/her work is accessed as described above and to be protected against infringement.

For additional information about the Linköping University Electronic Press and its procedures for publication and for assurance of document integrity, please refer to its WWW homepage:

<http://www.ep.liu.se/>

© Jenny Johansson and Mikaela Waller  
Linköping, 23rd September 2005